

# Master Thesis

## Evaluation of Hydrophobic Coated Glass Beads for Utilization in Gravel pack



Written by:

Mohsen Fakhari, MSc

University Advisor:

Univ.-Prof. Dr.mont.Herbert Hofstätter

Matriculation Number:

1235489

OMV Advisor:

Dip-Ing Robert Maier

Leoben,

02.12.2014

## **EIDESSTATTLICHE ERKLÄRUNG**

Ich erkläre an Eides statt, dass ich die vorliegende master thesis selbständig und ohne fremde Hilfe verfasst, andere als die angegebenen Quellen und Hilfsmittel nicht benutzt und die den benutzten Quellen wörtlich und inhaltlich entnommenen Stellen als solche erkenntlich gemacht habe.

## **AFFIDAVIT**

I hereby declare that the content of this work is my own composition and has not been submitted previously for any higher degree. All extracts have been distinguished using quoted references and all information sources have been acknowledged.

## Kurzfassung

Die Blockade des Bohrlochs aufgrund von Kalkablagerung, welche oft zur Beeinträchtigung der Förderung von Kohlenwasserstoffen führt, ist eines der größten Probleme im Sand- Control- Bereich. In der Industrie sind bereits viele Verfahren für die Beseitigung bekannt. Diese sind jedoch meistens zeitaufwändig und durchaus kostenspielig. Firmen und Forschungsinstitute bestreben günstigere Alternativen, die die Ablagerung von Kalk nicht nur beseitigen, sondern auch vorbeugen.

Diese Master Thesis untersucht, die Eignung von Glaskugeln für diesen Einsatz. Das Verfahren wird bei Sand- Control- Packs wie Gravel Packs (GP), High Rate Water Packs (HRWP) und Frack Packs (FP) eingesetzt.

Durch verschiedene Laborveruche wird gezeigt, wie inerte Glaskugeln mit glatter Oberfläche einen positiven Einfluss auf die Durchlässigkeit haben. Ein weiterführender Schritt in der Entwicklung ist die Einführung von hydrophobischer Beschichtung der Glaskugeln, welche die Effektivität noch weiter erhöht.

Weiters wird das Ausmaß von Kalkablagerung für verschiedene Proppant- Packs unter dynamischen Bedingungen im Rahmen von zusätzlichen Laborexperimenten simuliert. Dies wird für unterschiedliche Druckwerte getestet. Anschließend wird die beobachtete Kalkablagerung mit einem Mikroskop analysiert. Darüber hinaus wird auch ein Versuch unter statischen Bedingungen durchgeführt, um weitere Informationen über die Hydrophobität der entwickelten Beschichtung zu erhalten.

Das Ziel war eine Alternative zu bereits verwendeten keramischen Körnern zu finden, die genauso leicht herstellbar sind. Aus diesem Grund fiel die Auswahl auf beschichtete bzw. unbeschichtete Glaskugeln in verschiedenen Größen. Dank der physikalischen Eigenschaften dieser, wird die Permeabilität erheblich erhöht. Außerdem verzögern sie die Entstehung von Kalkablagerung.

Das Projekt wurde in enger Zusammenarbeit mit der Montanuniversität Leoben, dem Forschungsinstitut Gänsendorf der OMV, Prof. H. Hofstätter und Robert Maier durchgeführt. Das Glasmaterial wurde von Swarco Company zur Verfügung gestellt.

## Abstract

Plugging of the downhole sand control installations by scaling, strongly impacts oil production. There are several time consuming and expensive techniques to remove and avoid this problem. However companies and research institutes are interested in cheaper ideas to prevent scaling and avoid production loss and costly conventional scale removal methods. The aim of this thesis is to investigate on the possibility to avoid or reduce scale precipitation by using the glass beads, to be used for sand control installations such as Gravel Packs (GP), High Rate Water Packs (HRWP) or Frack Packs (FP). Laboratory experiments were designed to evaluate the positive impact of inert proppant with smooth surface as well as to demonstrate the improvement of this effect by coating the glass beads with a hydrophobic layer.

Simple laboratory methods are employed to measure the scaling trend on various proppant packs in a dynamic mode to simulate closer bottom hole flow conditions. The pressure values obtained from the experiments were compared and the observed scale build up, investigated visually under the microscope. Further a static experiment was developed as a supplementary information about affectivity of hydrophobic coating material. The choice of proppants was restricted to the man-made ceramic proppant commonly used by companies and coated and non-coated glass beads, in terms both material and size. To that end, material consisted of ceramic and both hydrophobic and normal glass.

One key conclusion is that because of physical properties, glass beads demonstrated significantly higher permeability than ceramic. In addition the experiment results implies affectivity of utilizing glass beads to defer plugging problem by scaling.

This project has been carried out in close cooperation with the Montanuniversität Leoben and OMV research centre in Gänserndorf as well as the respective supervisors Prof.H. Hofstätter and Robert Maier. The glass material was kindly provided by Swarco Company.

## List of Tables

Table 1 - Consequences of sand production in reservoir, subsurface and surface equipment [1].....	2
Table 2 - Physical properties of sand and fine (clay) [2, p. 2].....	2
Table 3 - A scale of grade and class terms for classic sediments. – Wentworth [3, p. 2].....	3
Table 4 - Water soluble scaling material [11] and [12].....	13
Table 5 - Gravel size analysis of glass beads with cumulative comparison in percentage .....	23
Table 6 - Composition analysis of normal quartz sand grains .....	28

## List of Figures

Figure 1-A stable arch is believed to form around the entrance to a perforation cavity [4].	4
Figure 2-Mohr's circle	5
Figure 3 - Sanding tendency is characterized from USC-porosity correlation on five reservoirs in Saudi Arabia [7]	6
Figure 4 - correlation between flow rate and amount of sand produced [7].	7
Figure 5 - the sand box.	9
Figure 6 - Evidence of no interaction with 12/20 mesh gravel [21].	10
Figure 7 - Evidence of hyperbolic decrease in all invaded zones with 20/40 mesh gravels.	10
Figure 8 - Evidence of combined internal bridging and single pore blocking mechanisms [21].	11
Figure 9 - Evidence of shallow internal bridging mechanism [9].	11
Figure 10 - Evidence of no invasion [12].	12
Figure 11- solubility of calcium carbonate as a function of PH [10]	14
Figure 12 –A portion of production history from one of the prolific wells in the Gullfaks field shows cyclic production impairment.	16
Figure 13 – EDTA chelate compound	17
Figure 14 - inhibitors are retained in the formation by either adsorbing to the pore walls or precipitating in the pore space.	18
Figure 15 – The gravels treated with the water based SMA hydrophobic material shows no indication of plugging during the test period [17].	19
Figure 16 - schematic illustration of a surfactant with hydrophobic and hydrophilic heads.	20
Figure 17 - Contact angle of a liquid on a surface	21
Figure 18 - An illustration of some of the parameters influencing the force needed for a drop to start sliding down a titled surface.	22
Figure 19 - the different wetting models (a) Wenzel and (b) Cassie-Baxter	22
Figure 20 - Appearance of glass beads. On the right side hydrophobic coated glass beads and on the left side Normal glass.	23
Figure 21- the cumulative size analysis of glass beads.	24
Figure 22 - Microscopic pictures of normal non-coated glass beads.	25
Figure 23 - Microscopic pictures of hydrophobic coated glass beads.	25
Figure 24 - 2 cc of distilled water is added to both types of glass beads.	26
Figure 25 - One droplet of water on the surface of hydrophobic glass beads.	26
Figure 26 - On the left side natural quartz sand and on the right side ceramic proppant.	27
Figure 27 - Normal quartz sand microscopic picture.	27
Figure 28 - Ceramic grains microscopic pictures.	27
Figure 29- Dry samples (on the top) and samples after adding water (down).	29
Figure 30 - The centrifugal pump (GRUNDFOS-TP-Vertical) on the right side and reciprocation pump (LC-20AT) on the left.	30
Figure 31 - Memmert UFE 500 (oven)	31
Figure 32 - The steel cell. With the 20 cm length steel cell	32
Figure 33 - Second steel cell with 1.18 cm diameter.	32
Figure 34 - MGCplus amplifier	33
Figure 35 - Scale - OHAUS EXPLORER	33
Figure 36 – Setup to measure permeability. P1 and P2 refer to inlet and outlet pressure respectively	35
Figure 37 - Pressure drop in ceramic permeability test	36
Figure 38 - Pressure drop of quartz gravel sands.	36
Figure 39 - Pressure drop through both hydrophobic coated and normal glass beads are the same.	37
Figure 40 - Compare permeability of different samples.	37
Figure 41 - Permeability collation of glass beads with ceramic.	38
Figure 42 – The 50% mixture of fluid A and B in concentrations of 1, 2, 3, 4 and 5 [gr/lit]	41
Figure 43 - Samples after 30 minutes heating at 80°C.	42
Figure 44 - Increasing ph in the mixture of 1.68 gr/l sodium bicarbonate and 1.47g/l of calcium chloride.	43
Figure 45 – The setup for precipitation test without heating	44

Figure 46 - Dynamic precipitation setup by heating.....	45
Figure 47 - The pressure increment because of calcium carbonate scaling. ....	46
Figure 48 - Ceramic grain after dynamic precipitation test in 60° centigrade. ....	47
Figure 49 - Calcium carbonate crystal on the surface of ceramic after dynamic precipitation test at 60° centigrade.....	48
Figure 50 - Precipitation and adherence of calcium carbonate on the surface of glass grain in dynamic test at 60° centigrade. ....	48
Figure 51 - Precipitation of calcium carbonate on the surface of glass in dynamic test at 60° centigrade.....	49
Figure 52 - Hydrophobic glass picture after dynamic precipitation test in 60° centigrade. ....	49
Figure 53 - Crystallization of calcium carbonate on the surface of ceramic grain after static test.....	50
Figure 54 - Microscopic picture of surface of ceramic grain after static precipitation test. ....	51
Figure 55 - Non-coated glass bead after static test. ....	51
Figure 56 - Microscopic photo of hydrophobic coated glass bead after static precipitation test. ....	52
Figure 57 - Effect of length on nucleation along the cell. ....	53
Figure 58 – Gibbs free energy .....	59
Figure 59- Schematic of heterogeneous nucleation relatove to Gibbs free energy.....	60
Figure 60 – Definition of shape category .....	61
Figure 61 - Visual chart for estimation of roundness and sphericity of particles .....	62



## Abbreviations

$\Delta P_{dd}$	Drawdown pressure
$\sigma_n$	Normal stress
$\emptyset$	Internal friction angle
$\Delta P$	Pressure Drop
A	Area
D	Darcy
$D_g$	Gravel diameter
$D_o$	Reference diameter
$D_s$	Formation sand diameter
FP	Frack pack
G	Gibbs free energy
GP	Gravel pack
K	Absolute permeability
$K_{sp}$	Solubility Product
L	Length
q	Flow rate
r	Radius
SSV	Surface safety valve
T	Temperature
t	time
UCS	Uniaxial compressive strength
$\theta$	Wetting contact angle
$\mu$	Viscosity
$\sigma$	Interfacial tension
$\tau$	Shear stress
$\phi$	Krumblin phi scale

## CONTENTS

1	Introduction .....	1
2	Sand Production .....	2
2.1	Definition of sand and fine characterizations .....	2
2.2	Sand production mechanisms .....	4
2.2.1	Rock mechanic failure and sand production .....	5
2.3	Sand control mechanisms: .....	7
3	Damage mechanisms of gravel packing .....	9
3.1	Invasion of sands and fines .....	9
3.2	Scaling problem .....	12
3.2.1	Precipitation of calcium carbonate .....	13
3.2.2	Calcium carbonate scale mechanisms in field .....	15
3.3	Literature review about scaling remediation in gravel packing .....	15
3.3.1	Chemical dissolution .....	16
3.3.2	Preventing Scale .....	17
4	Innovative hydrophobic glass bead gravels utilization to control the scaling problem .....	20
4.1	Introduction .....	20
4.1.1	Hydrophobicity .....	20
4.2	Apparent physical properties of samples .....	23
4.2.1	Tools and equipments .....	29
4.3	Permeability evaluation with base fluid .....	34
4.3.1	Permeability .....	34
4.3.2	Process and test setup _ Base permeability .....	34
4.3.3	Tools and equipment _ Base permeability .....	35
4.3.4	Tests and results .....	35
4.3.5	Discussion .....	37
4.4	Precipitation Tests .....	39
4.4.1	laboratory experiments for precipitation of calcium carbonate (pcc) .....	39
4.4.2	Preparation of precipitation process .....	40
4.4.3	Precipitation of calcium carbonate in gravel packs- Dynamic Tests .....	43
4.4.4	Microscopic evaluations for dynamic test .....	47
4.4.5	Microscopic evaluation of static test .....	50
4.4.6	Discussion .....	52
5	Conclusion and future directions .....	54
5.1	Conclusion .....	54
5.2	Future Directions: .....	54
6	References .....	56

7	Appendices .....	59
7.1	Appendix A .....	59
7.2	Appendix B .....	61

# 1 INTRODUCTION

Scaling is one of the most important problems in oil industry that can coat and plug perforations, gravel packs and downhole completion equipment and even surface facilities. This problem occurs after a period of production, depends on formation and production condition, and usually operators apply chemical solutions like hydrochloric acid to solve the problem. Although chemical dissolution is an easy remedial but from economical point of view, scale removal is an expensive approach. The high costs of regular interventions makes operators interested in scale preventing methods.

The objective of this thesis is to evaluate the ability of glass beads as an inert proppant material, to be used for sand control installations such as Gravel Packs (GP), High Rate Water Packs (HRWP) or Frack Packs (FP), to avoid or at least reduce scale precipitation. Secondly it was investigated if the expected effect can be improved by coating this type of proppants with hydrophobic material. To evaluate the “water repelling” effect of the glass proppant and hydrophobic coated glass proppant a test procedure was developed which compared scale precipitation inside a proppant pack to man-made ceramic gravel material used in the industry.

The process of scale precipitation generally occurs over longer time in the fields, therefore it was important to design a process, which allowed for representative and reliable results considering laboratory and time limitations.

In the first step, physical properties of samples consisting of, shape, sphericity, size and hydrophobicity, were evaluated. Second a test setup was designed to measure the permeability of proppant packs based on Darcy equation.

Further sections of the thesis give insight in literatures about scaling theory and past experiments relative to precipitation of calcium carbonate in laboratory, the preparations and reasons for decisions in regards to the materials and evaluation set up chosen, the established evaluation criteria, the laboratory work, the test results and the conclusions drawn.

To design the precipitation setup some factors were considered. First, the setup was designed to allow scaling in dynamic flow condition, because dynamic setup makes it possible to monitor and understand trends and rates of scaling, additionally it mirrors perfectly downhole flow conditions. Secondly is try to design a setup by hiring minimum number of variables, this could simplify the analysis and make the results more reliable.

On the other hand, static tests represents an additional information about the hydrophobicity effect of coated glass.

Finally the precipitation mode and actual method of pore throat reduction was investigated under the microscope and determined by visible judgement.

## 2 SAND PRODUCTION

Sand production is one of the oldest controversial problems in the oil and gas industry. Although sanding most likely occurs in shallow poor consolidated formations of Tertiary age, some other deep formations with 12000 feet or more may encounter this problem.

In unconsolidated formations with high rates of sand production if the flow rate in the wellbore is not sufficient to transport produced sand to surface, then it would accumulate and shutoff the wellbore. On the other hand, if the velocity is sufficient to transport the sands, erosion on the subsurface and surface equipment takes place. The replacement process of such subsurface tools is expensive due to production loss and cost of material.

In addition, produced sand can also cause additional significant cost for logistic and disposal, particularly on offshore sites.

Another important problem is the formation instability, caused by creation of void spaces in formation as a result of sand production. It will cause collapse in the wellbore and leave the casing unsupported behind. Table 1 shows the consequences of sand production in all three divisions of reservoir, subsurface facility and surface installations.

Table 1 - Consequences of sand production in reservoir, subsurface and surface equipment [1]

Area	Problem	Effect
Reservoir	Wellbore fill	<ul style="list-style-type: none"> <li>• Restricted access to production interval</li> <li>• Loss of productivity</li> <li>• Loss of reserve</li> </ul>
Subsurface Equipment	Sand fouling	<ul style="list-style-type: none"> <li>• SSSV not operation</li> <li>• Difficult wire line operation</li> </ul>
	Erosion	<ul style="list-style-type: none"> <li>• Equipment replacement</li> <li>• Equipment failure</li> </ul>
Surface Installation	Sand accumulation	<ul style="list-style-type: none"> <li>• Malfunctioning of control equipment</li> <li>• Unscheduled shut down</li> </ul>
	Erosion	<ul style="list-style-type: none"> <li>• Deferred production</li> <li>• Sand separation and disposal</li> </ul>

### 2.1 DEFINITION OF SAND AND FINE CHARACTERIZATIONS

Naturally produced solids divide into two types of sands and fines. Sands are detrital grains of mineral oxides (like SiO<sub>2</sub>) which are defined as load bearing solids of the formation, however fines or clay are not part of mechanical structure of the formation. Physical properties of sand and fine are shown in Table 2.

Table 2 - Physical properties of sand and fine (clay) [2, p. 2]

Property	Sand	Clay
Specific Gravity	2.5-2.9	2.6-2.8
Shape Factor	0.2-0.5	0.1-0.3
Size Range (µm)	50-1000	5-30
Concentration (ppmv)	5-100	< 1

The most common produced sand is silica based, so the gravity would be around 2.65. These material have poor shape factor (see in Appendix B) that shows the high angularity.

While fine materials have the same gravity, but they are smaller in size. Based on Byrne, et al. (2010) [3], there are two points of view to define fines, geological and engineering. In geological definition, all different properties consist of composition, size and shape of particles considered, however engineers just tend to use size based methods. In the geological point of view, fines are those particles with the size less than 2 microns, while Engineers define fines, all particle sizes which usually can be produced without harming downhole or surface installations.

The grain size generally considered acceptable is less than 45 microns. The origin of this value is not completely clear but it could arise from one of these two explanations:

- A 325 mesh screen or 45 micron is the finest manufactured sieve aperture size, so everything pass through this sieve was difficult to be characterized in dry sieve analysis and classified as fine.
- The average pore size of the 40/60 mesh gravel that is smallest commonly used gravel pack gravel, is about 45 microns.

Table 3 shows the sediment classification on size provided by Wentworth. That sand and clay are defined based on their sizes.

Table 3 - A scale of grade and class terms for classic sediments. – Wentworth [3, p. 2]

$\phi$ scale	Size range (metric)	Size range (approx. inches)	Aggregate name (Wentworth Class)	Other names
-8 <	256 mm <	10.1 in <	<u>Boulder</u>	---
-6 to -8	64–256 mm	2.5–10.1 in	<u>Cobble</u>	---
-5 to -6	32–64 mm	1.26–2.5 in	<u>Very coarse gravel</u>	<u>Pebble</u>
-4 to -5	16–32 mm	0.63–1.26 in	Coarse gravel	Pebble
-3 to -4	8–16 mm	0.31–0.63 in	Medium gravel	Pebble
-2 to -3	4–8 mm	0.157–0.31 in	Fine gravel	Pebble
-1 to -2	2–4 mm	0.079–0.157 in	Very fine gravel	<u>Granule</u>
0 to -1	1–2 mm	0.039–0.079 in	<u>Very coarse sand</u>	---
1 to 0	½–1 mm	0.020–0.039 in	Coarse sand	---
2 to 1	¼–½ mm	0.010–0.020 in	Medium sand	---
3 to 2	125–250 $\mu\text{m}$	0.0049–0.010 in	Fine sand	---
4 to 3	62.5–125 $\mu\text{m}$	0.0025–0.0049 in	Very fine sand	---
8 to 4	3.90625–62.5 $\mu\text{m}$	0.00015–0.0025 in	<u>Silt</u>	<u>Mud</u>
> 8	< 3.90625 $\mu\text{m}$	< 0.00015 in	<u>Clay</u>	Mud
> 10	< 1 $\mu\text{m}$	< 0.000039 in	<u>Colloid</u>	Mud

The Krumbein phi scale ( $\phi$ ), created by Wentworth and computed by the equation below:

$$\phi = -\log_2 D/D_0 \quad (1)$$

$\phi$  is the Krumbein phi scale

$D$  is the diameter of particle

$D_0$  is a reference diameter, equal to 1 mm

## 2.2 SAND PRODUCTION MECHANISMS

Throughout the world a significant number of high reserves hydrocarbon formations are unconsolidated sandstones. Most of these formations are composed of sand, silt and clay. The smaller sand and clay particles, generally less than 45 microns are called “fines”. These particles have the tendency to get released when fluids are producing. Well completions are usually designed to allow these fines (that comes from reservoir) to be produced, because on the contrary they will plug the pores and reduce reservoir or gravel pack permeability. Bigger grain sized particles must be controlled, since producing them makes the well bore unstable and finally collapse occurs.

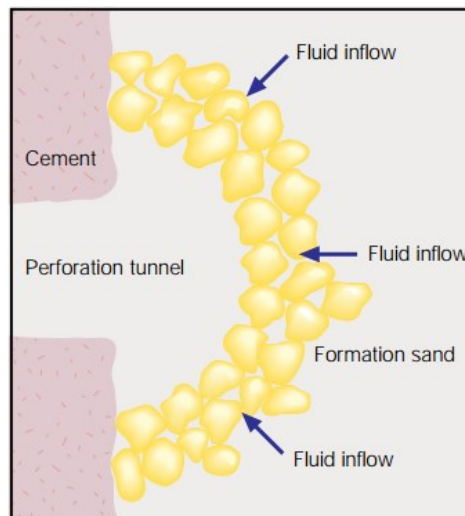


Figure 1 - A stable arch is believed to form around the entrance to a perforation cavity. This arch remain stable as long as flow rate and draw down are constant. By changing flow rate the arch will collapses and new one forms once flow got stable [4]

In highly unconsolidated formations, sand production observed due to drag force and gas turbulence, even in first production. However in some better consolidated formations, sanding may start as a result of changing in production flow rate. Fluctuation in production rate may affect perforation cavity stability and in some cases hamper the creation and maintenance of sand arches that is stable in constant rates (Figure 1).

Furthermore the sand producing tendency in the formation increases by starting water influx, since water cause reduction in the grain to grain cementation [4, p. 2].

Main reasons and mechanisms of sand production are referred to rate of production, viscosity of the fluid and weakness of wellbore. The main reasons of sand production can categorize into following four factors [5, p. 36]:

- Drag force of flowing fluid is proportional to flow rate and fluid viscosity.
- Reduction in formation strength often associated with water production due to dissolving the cementing material.
- Reduction of relative oil permeability due to increment of water saturation.
- Declining reservoir pressure that reduces compaction force and disturb cementation between grains.

### 2.2.1 ROCK MECHANIC FAILURE AND SAND PRODUCTION

The important factors affecting mechanically failure in reservoir rock consist of rock strength, effective stress (principal stress minus pore pressure) and stresses introduced by drilling, completion and production.

Uniaxial and triaxial stress tests can demonstrate the failure curve and rock strength. The shear and normal stress in this failure curve can be determined by Mohr- Coulomb failure model (Figure 2). This model relates the principal stresses and pore pressure to the cohesion and internal friction angle of the rock.

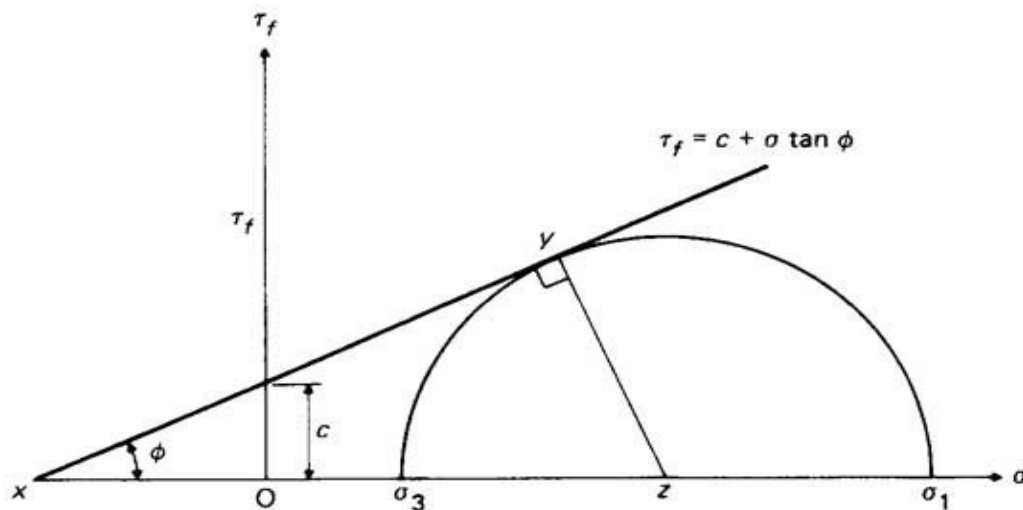


Figure 2-Mohr's circle, the XY line demonstrate the failure condition that material will fail in shear. Mohr's circle also provide the normal stress ( $\sigma_n$ ) and shear stress ( $\tau$ ) and internal friction angle ( $\phi$ ). [6, p. 3]

Cohesion is influenced by the degree of cementation of the rock, so well cemented and consolidated rocks have greater cohesion. Internal friction angle is influenced by the volume fraction of hard particles like quartz and feldspar grains in rock.

During the production both drawdown and depletion can result sand production because of shear failure. Drawdown increases the effective stress around the wellbore and if it exceed the rock's strength, consequences the sand production. Depletion also causes changes in in-situ



stresses in the reservoir and makes higher shear stress around the bore hole by decreasing the pore pressure and increasing the effective stress.

Tensile failure occur in weak sandstones as a result of drawdown and high flow rate production. This kind of sand productions are relatively low and stabilizes within the time. [6]

Research results on wells with sanding problem can clearly demonstrate that geomechanical parameters play a significant role in sand production. Abbas et al. (2002) analysed five sandstone reservoirs in Saudi Arabia categorized based on uniaxial compressive strength (UCS). Two of these reservoirs have, UCS less than 6000 psi and porosity greater than 13% (shown by blue and brown in Figure 3).

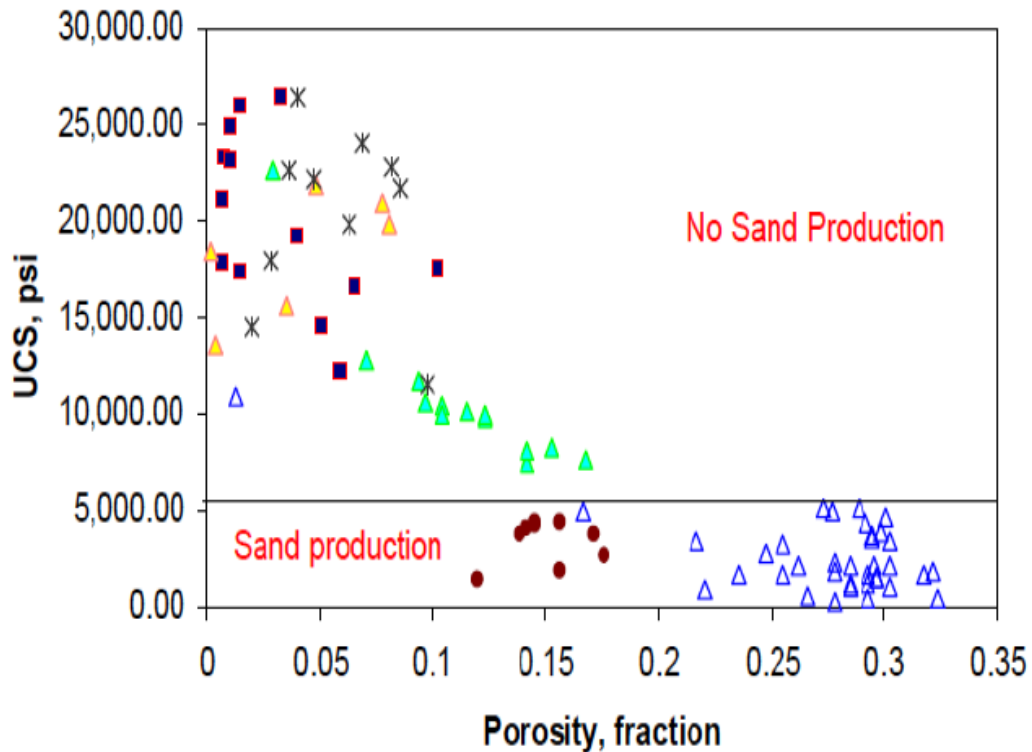


Figure 3 - Sanding tendency is characterized from USC-porosity correlation on five reservoirs in Saudi Arabia [7]

As mentioned above drawdown also causes shear failure and sanding, to control it a critical flow

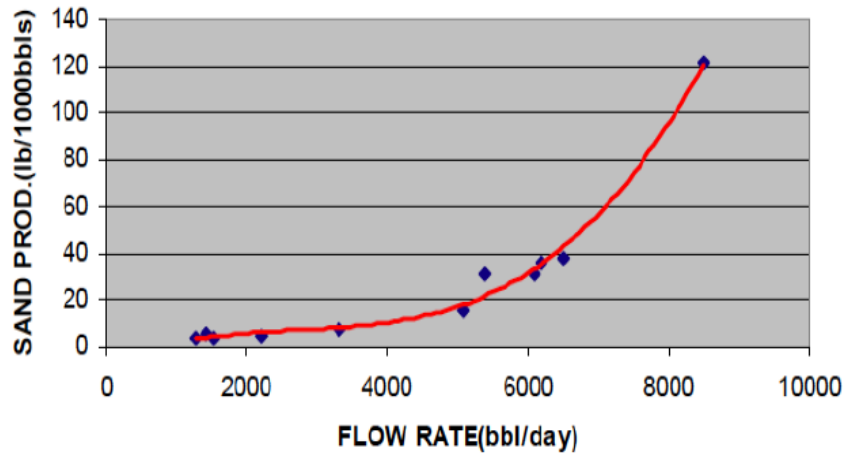


Figure 4 - SAFANIYA field sand production, correlation between flow rate and amount of sand produced [7].

rate interval need to be defined. Figure 4 demonstrate a field correlation between the wellhead pressure and the amount of sand production in SAFANIA oil field. There are some geomechanical based methods to find the critical flowrate that in these methods, if drawdown pressure exceed uniaxial compressive strenght causes failure and results sand production. Field experiences showed that the critical point for drawdown pressure is the half of UCS [7]:

$$\Delta P_{dd} = 0.5 \times C_o \quad (2)$$

Where  $C_o$ , is UCS and  $\Delta P_{dd}$  is drawdown pressure.

### 2.3 SAND CONTROL MECHANISMS:

Basically there are three main mechanisms to control sand production:

#### 1. Reduction of drag forces

It is considered as the cheapest and most effective solutions for sanding problem. The drag force in the wellbore is generally related to flow rate and conductivity of near wellbore formation. To increasing the near well conductivity, well completion play a significant role. Providing high density and large perforation throughout the producing section is an important issue.

Another alternative is restricting production rate, although this is an effective method, is often regulated by market demand and economics. To estimate the maximum production rate (limited by critical flow rate due to sanding) it is possible to use bean up test. Bean-up refers to the gradually increasing the choke size to open up a well for production. When the critical range has reached the sand production increases and goes in the highest level, then production rate must be reduced below the critical range. It takes some months to understand the maximum production level for wells with or without sand control mechanisms. [8]

#### 2. Mechanical methods of sand control

It is the most common approach that include downhole devices to bridge or filter the produced fluid. In this method usually gravel pack placed in the downhole to hold formation sand in place.

Also installation of Stand-alone slotted liners or screens is a common technique to control sanding.

3. In-Situ chemical consolidation methods

Chemicals injected into the unconsolidated formation, that provide grain to grain cementation and increasing the formation strength at the near wellbore zone..

### 3 DAMAGE MECHANISMS OF GRAVEL PACKING

Corresponding to the explanation in the previous chapter, gravel packing is one of the most well-known mechanical methods to control sand production. Although it is a useful method to control sanding, but during production, because of mechanical and chemical damages, gravel pack's permeability will reduce dramatically. Main damages that can reduce the permeability of gravel packs are sand invasion and scaling.

#### 3.1 INVASION OF SANDS AND FINES

Gravel packs are installed to control the migration of load-bearing formation sand from unconsolidated reservoirs, but any gravel pack itself gradually or instantaneously (depend the production and well condition) get plugged by sand and fine migration from both unconsolidated reservoirs and fluid's injection into the wellbore. Therefore in designing gravel packs the important factor of plugging by fine invasion need to be considered. To achieve this objective a strict criteria should define for gravel sizing. Current common sizing instruction in the oil industry is the Saucier method. In the Saucier formula gravel size is chosen based on the mean size of formation sand. But since the effect of flow and poorly consolidated formations are not considered, in large number of installed gravel packs, significant fines production is reported. Depending on the depositional environment, different sands with same sizes may have lithology and stratigraphic features that causes different sanding rates. While based on the Saucier method same gravel packs will be designed for both of them.

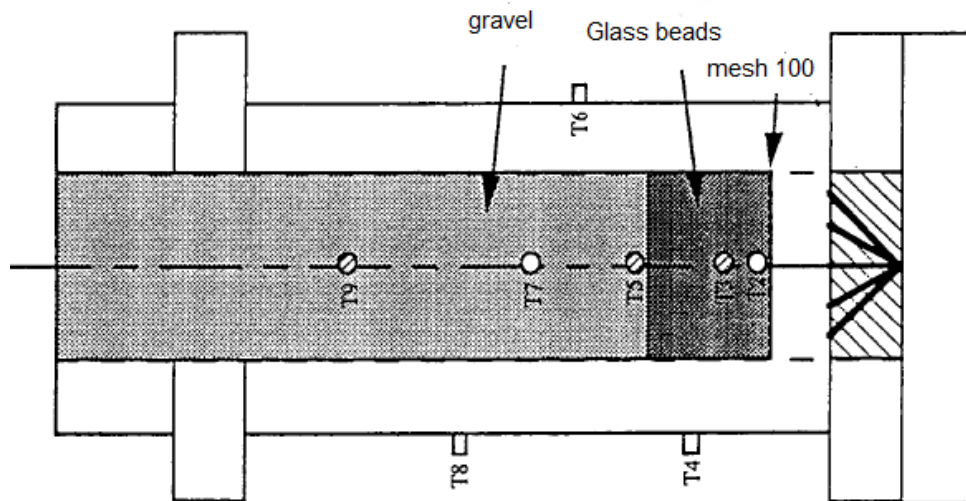


Figure 5 - The sand box. The cell is filled with fine glass beads (50 to 70 micron) from T1 to T5 gravel packs. and the rest is filled with common sands [9].

ed with eight strain gauge transducers radially spaced at specific intervals for monitoring of pressure drop. Then the slurry containing sand and fines were injected into the cell. Therefore by monitoring rate and pressure drop, permeability could be calculated. Schematic of the cell with the transducers is shown in Figure 5.

They categorized sand invasion into five different scenarios with defining five different size ratio of gravel over formation sands ( $D_g/D_s$ ):

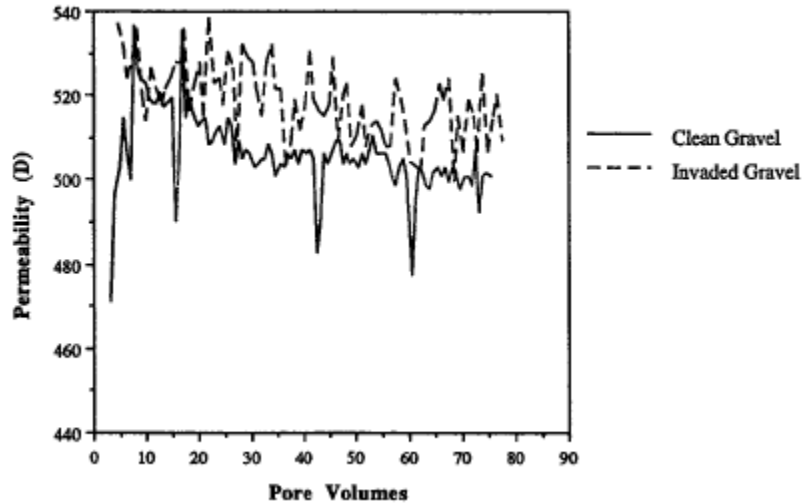


Figure 6 - Evidence of no interaction with 12/20 mesh gravel [9].

1. No interaction: for gravel size with more than 15 times larger than formation sands. Fines are free to produce due to very large pore existing in the gravel pack. The Figure 6 represents the trend of permeability reduction against injected pore volume.
2. Pore filling: this mechanism is for gravel-sand size ratio of  $10 < D_g/D_s < 15$  and represent the gradual deposition of particles into pore spaces, resulting a hyperbolic reduction of permeability with time. Different permeabilities in Figure 7 are because of two types of gravels are used (can be seen in Figure 5).

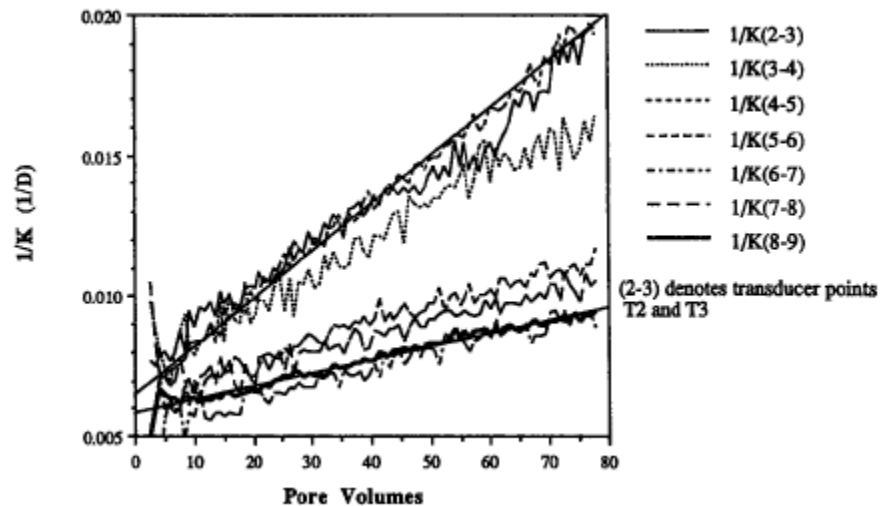
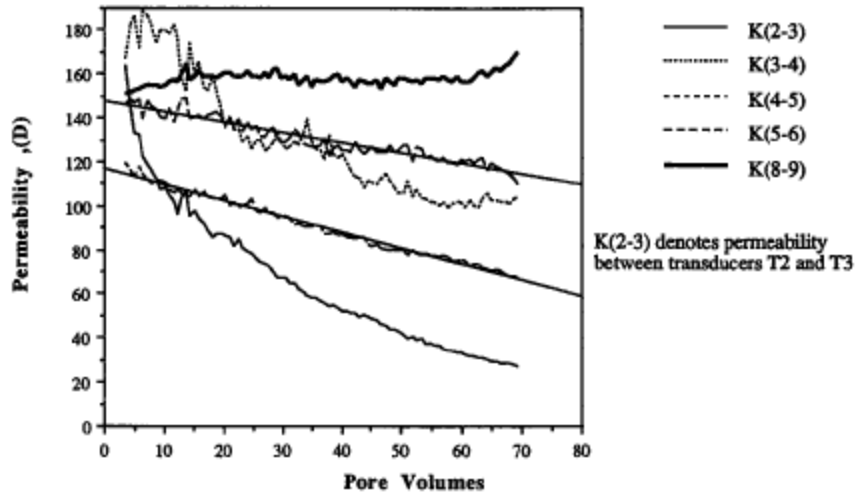


Figure 7 - Evidence of hyperbolic decrease in all invaded zones with 20/40 mesh gravels. The  $k(2-3)$  means permeability between T2 and T3 [9].



3. Combined internal bridging and single pore blocking mechanisms [9]. Particles were found to be larger than the pore size or to  $6.5 < D_g/D_s < 10$ , (Figure 8).
4. Shallow internal bridging: the phenomena is referred to the gravel-sand size ratio of  $5 < D_g/D_s < 6.5$  that makes a shallower pugging than the last mechanism.

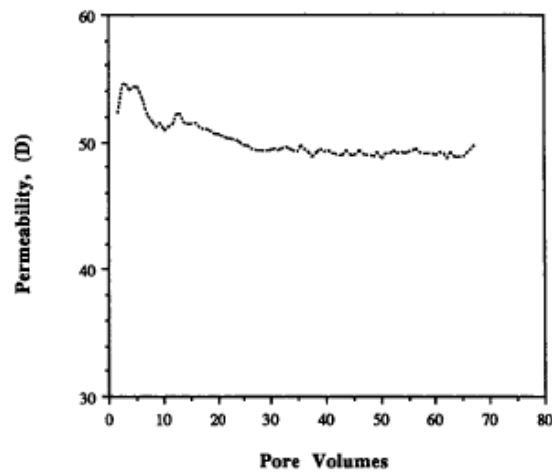


Figure 9 - Evidence of shallow internal bridging mechanism [9]

5. No invasion: tested by ratio of  $D_g/D_s < 5$  and applies for cases of absolute fine stoppage by gravel pack relative to small pore size in gravel packs (Figure 10).

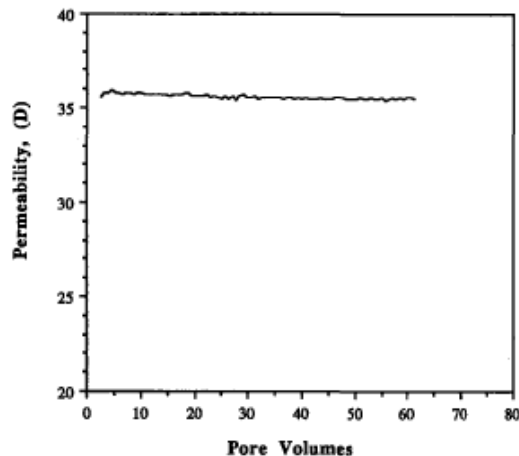


Figure 10 - Evidence of no invasion [9].

Test results admit the size interval introduced by Saucier. The size ratio between 5 to 6 times bigger gravel to formation sand give the best permeability regarding the shallow fine invasion. Although with the ratio of less than 5 there is no invasion, Figure 10, but because of smaller pore throat the permeability reduce dramatically. This low permeability has the same effect as pore plugging by sand invasion. Also in ratios greater than 6, there is no sand invasion because large pore spaces let the sand to be produced.

### 3.2 SCALING PROBLEM

Scaling is one of the most controversial problems in oil fields which can deposit in downhole and surface facilities, thereby clogging the wellbore and prevent the production. The deposited scale formation is such as precipitated layer in tea kettles at home. Scales comes from reservoir water and forms a solid layer in formation pores which results reduction in porosity and permeability. Since most of the minerals are soluble in water, reservoir water can carry a large quantity of scaling materials. As a result reservoir water becomes enriched with variety of ions and mineral where some of them are at the saturation limit. By temperature and pressure fluctuation the thermodynamic equilibrium changes and solubility state converts to oversaturated level. Different minerals have various trends regarding solubility dependency with pressure and temperature, typically, temperature increasing causes increment in solubility but for calcite it is inverse.

Scaling starts by formation of unstable cluster atoms that form small seeds which are created because of sudden local fluctuation in the equilibrium ion concentrations, called "homogeneous nucleation". Adding more ions to crystal surfaces needs energy that comes from superheating, but increasing the size of crystals causes a decrease in the requirement of free energy and finally when the radius of precipitated material exceeds the certain level the free energy becomes negative which is in favour of crystal growing.

The same process as described above is happening but not in the same condition, called "heterogeneous nucleation". In this type of nucleation, crystals tend to growth on pre-existing fluid boundary such as pipe surface or perforations or gravel packs. This type of nucleation is easier and faster, because the required free energy for nucleation is less. The nucleation was

described by Gibbs. A more detailed explanation of this phenomena and the required energy, called “Gibbs energy” is given in Appendix A.

In the oil fields there are some common reasons for scaling that it is possible to categorize them into four different scenarios [10]:

1. Incompatible mixing: during the water flooding enhanced recovery, eventually injected water and formation water are not compatible and cause scaling. For example, when Sea water is used for flooding it happens that barium or calcium sulphate is formed because Sea water usually contains  $\text{SO}_4^{2-}$  in high concentrations; while reservoir water is often rich in calcium and barium ions.
2. Self-scaling: fluctuations in pressure, temperature and PH, changes the thermodynamic equilibrium in the fluid and reduce the solubility limit. Calcium carbonate and sulphate are the common scales which occur by this mechanism.
3. Evaporation-induced scale: during the production of wet gas by decreasing hydrostatic pressure in tubular, the volume of hydrocarbon gas expands and hot brine phase (since it is wet gas contain brine) evaporates. As a result the dissolve ions in the brine remains on the tube surface.
4. Gas flooding: for instance by injection of  $\text{CO}_2$  for enhance oil recovery. When this gas penetrates into the reservoir water, makes it acidic and dissolves calcite in the formation. By pressure drop during the production, carbon dioxide breaks out of the solution and pH increases which causes carbonate scale to precipitate.

### 3.2.1 PRECIPITATION OF CALCIUM CARBONATE

Generally compositions of scales in the oil fields consist of various inorganic materials, Table 4 shows the general soluble minerals at reservoir water according to their concentrations.

Based on this fact, calcium carbonate is the most common scaling material. This type of scale was selected to be used for evaluation of precipitation tendency in this thesis.

Table 4 - Water soluble scaling material [11] and [12]

Mineral	Formula
Calcite	$\text{CaCO}_3$
Aragonite	$\text{CaCO}_3$
Vaterite	$\text{CaCO}_3$
Anhydrite	$\text{CaSO}_4$
Gypsum	$\text{CaSO}_4$
Barite	$\text{BaSO}_4$
Celestite	$\text{SrSO}_4$
Mackinawite	$\text{FeS}$
Pyrite	$\text{FeS}_2$
Halite	$\text{NaCl}$
Fluorite	$\text{CaF}_2$
Sphaerlite	$\text{ZnS}$
Galena	$\text{PbS}$

Generally by changing the thermodynamic variables, the solubility level of calcium carbonate in reservoir water changes and accordingly precipitation takes place.



To define the solubility state of calcium carbonate in water, the solubility equilibrium is used, that shows the dynamic equilibrium between the solid and solution phases. When the equilibrium established, the solution is saturated. For calcium carbonate it is described by the solubility product  $K_{sp}$ , which shows the equilibrium between  $Ca^{2+}$  and  $CO_3^{2-}$ :

$$K_{sp} = Y_{Ca} [Ca^{2+}] Y_{CO_3} [CO_3^{2-}] \quad (3)$$

In pure water at 25 °C the  $K_{sp}$  is  $4.8 \times 10^{-9}$  moles/lit, that means about 6.9 mg in 1 liter. Temperature has an inverse relationship with solubility (solubility decreases by increasing temperature). One reported relationship for this temperature dependency [13], experimentally determined between 32 and 180 °F, is given as:

$$\frac{K_{SP,f}}{K_{SP,i}} = 6.57 \times 10^{-3} (T_i - T_f) \quad (4)$$

Where  $T_i$  and  $T_f$  are respectively the initial temperature 32°F and the final temperature 180°F, that solubility of carbonate calcium at  $T_f$  drop to about 3 mg in 1 liter of pure water.

On the other hand, pH controls the level of present  $CO_3^{2-}$  and consequently effect on solubility. In Figure 11, the pH dependency of solubility of calcium carbonate shows that from pH < 7, increasing pH dramatically reduces  $CaCO_3$  solubility, however from pH > 10.5 there is little changes in solubility. [14]

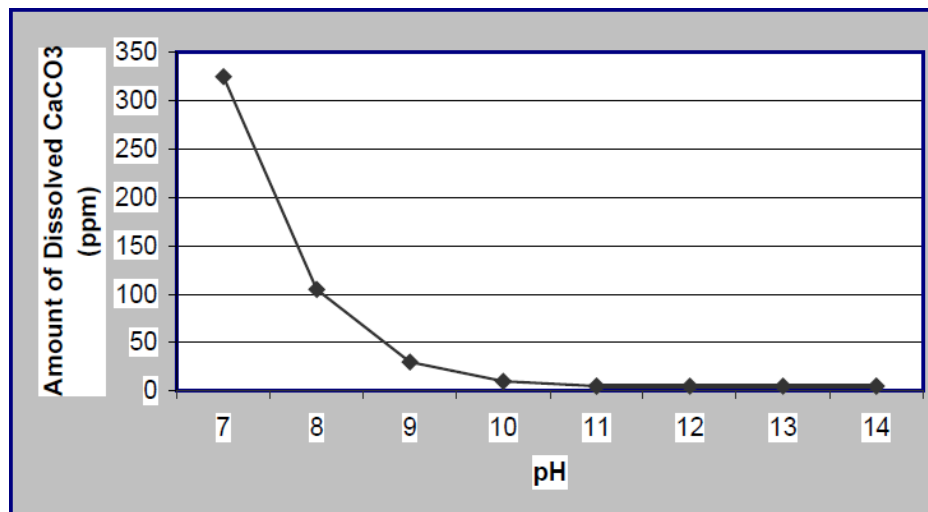
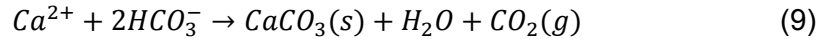


Figure 11- Solubility of calcium carbonate as a function of PH [14]

Derivation of chemical reactions in formation of calcium carbonate, consist of several steps. As it can be seen in equation 5,  $CO_2$ , as a free gas reacts with brine and forms carbonic acid ( $H_2CO_3$ ) but this carbonic acid is not stable and forms bicarbonate ( $HCO_3^-$ ) and carbonate ( $CO_3^{2-}$ ), which is described in equation 6 and 7. By existence of calcium cations dissolved in the water, according to equation 8 and 9, calcium reacts with carbonate and bicarbonate and produce  $CaCO_3$ .





But the solubility product of equation 7 is insignificant in compare with equation 6 as can be seen in equations 10 and 11.

$$k_1 = \frac{[H^+][HCO_3^-]}{[H_2CO_3]} = 4.2 \times 10^{-7} \left(\frac{moles}{l}\right)^2 \quad (10)$$

$$k_2 = \frac{[CO_3^{2-}][H^+]}{[H_2CO_3]} = 4.8 \times 10^{-11} \left(\frac{moles}{l}\right)^2 \quad (11)$$

Therefore reaction 8 can be ignored and reaction 9 taken as the common reaction that takes place in oil wells. Corresponding to these steps the precipitation of carbonate calcium occurs as the solution becomes supersaturated through lowering the CO<sub>2</sub> partial pressure [15].

### 3.2.2 CALCIUM CARBONATE SCALE MECHANISMS IN THE FIELD

Calcium carbonate will generate from brine or water during field operations nevertheless scaling mostly occurs in the presence of three phase fluid. It means the PVT behaviour of these three phases have an impact on precipitation of calcium carbonate.

O.J.Veter et al. (1987), investigated on practical mechanisms of CaCO<sub>3</sub> formation on fifteen different wells based on their PVT behaviour. The reservoir was considered without any free gas phase, when it is under static condition (no flow) there was no precipitation observed. But when the reservoir started production, even if the pressure was more than the bubble point, there was a small amount of scaling. This scaling was related to pressure reduction because the decrease of pressure, caused a decrease in the solubility of CaCO<sub>3</sub>.

Therefore by producing from reservoir soon or later the pressure in the well bore or reservoir, will become less than the bubble point in one of the three phases. As soon as the pressure drop from bubble point, the dissolved gas in both oil and brine phases will flashing. The flashing gas may contain CO<sub>2</sub> that by reduction of it in both phases the pH will increase, and the calcium carbonate precipitation will occur. The amount of CO<sub>2</sub> remaining within the brine phase depends on numerous thermodynamic variables, like temperature, pressure, partial pressure of CO<sub>2</sub> in the system, total amount of CO<sub>2</sub> in both oil and water phase [16].

### 3.3 LITERATURE REVIEW ABOUT SCALING REMEDIATION IN GRAVEL PACKING

In scaling removal or scale remediation two factors of time and non-damaging methods have to be taken into account. Since in most of the techniques the well has to be shut in (no production) during work over, the remedial processes have to be quick. Secondly the techniques applied have to be non-damaging to the wellbore. In the following section there is a review on different methods to remove and avoid scaling.

### 3.3.1 CHEMICAL DISSOLUTION

Chemical scale removal is generally the cheapest method. Dissolving calcium carbonate in hydrochloric acid is the most well-known scale removal techniques. While carbonate minerals are highly soluble in hydrochloric acid and can be easily dissolved, Sulphate scales are hard and have a very low acid solubility.

The efficiency and speed of chemical treatments are controlled by the ratio of scale surface to injected chemical. Therefore the reaction of chemical scale removal fluids in small surface area to volume like in thick, non-porous sheets of scale is usually slow. However in porous material like extremely thin plates of scales, reaction is relatively quick.

On the other hand, although hydrochloric acid is the cheapest and first choice for treatment of calcium carbonate (which is the most common scaling compound), it hides a problem. After scale removing by acid, the growth and reformation of remained crystals will occur again. A field study evaluated matrix stimulations with acid in the North Sea, Figure 12, clearly shows and confirms that carbonate precipitation in gravel packs was the primary damage mechanism causing recurring production losses in the wells.

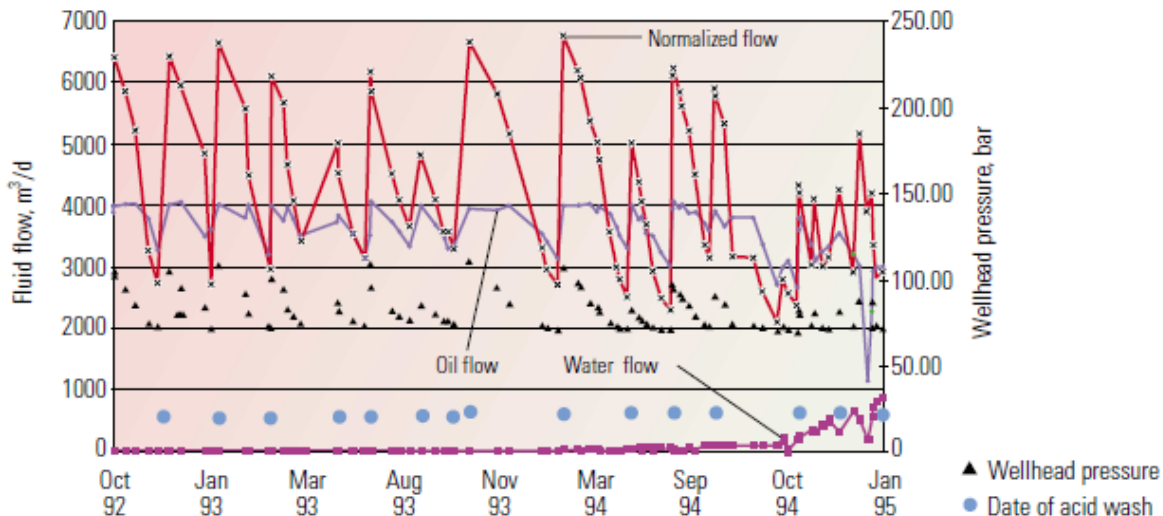


Figure 12 –A portion of production history from one of the prolific wells in the Gullfaks field shows cyclic production impairment. The normalized curve shows the large and immediate impact of multiple acid treatments (indicated by blue circles) and the subsequent loss in well productivity within one to three months afterwards that indicating recurring scale precipitation [10].

To break the cyclic precipitation of scale, some other chemicals introduced that can chelate calcium carbonate. Ethylene Diamene Tetra Acetic acid (EDTA) was an early candidate to improve chemical removal ability that surround the unwanted ions in solution and did not let it grow and reform scales again, Figure 13. Although EDTA is slower and more expensive than HCL, it compensates the recurring precipitation problem and also is effective on non-carbonate scale removal.

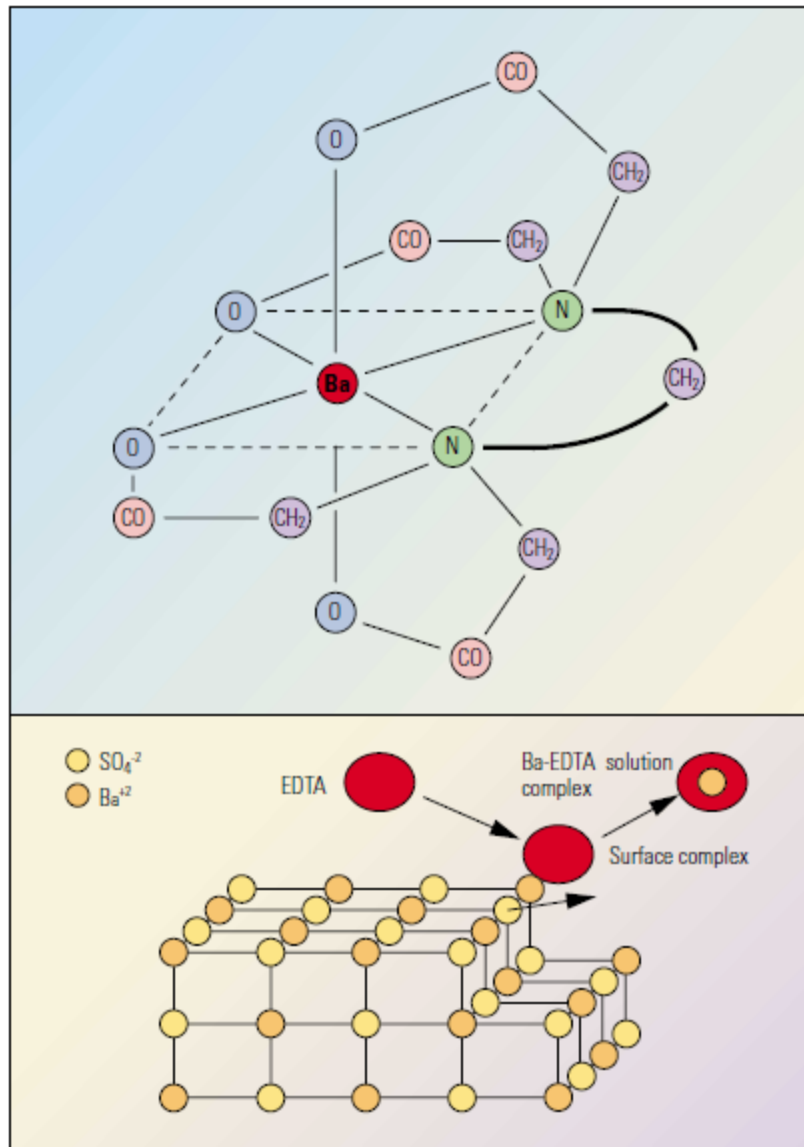


Figure 13 – EDTA chelate compound. Chelating agents are used to lock up unwanted ions in solution. An EDTA molecule shares electrons from oxygen and nitrogen atoms with barium ions, forming a barium-EDTA chelate compound (upper picture). The chelating process can help to dissolve solid barium sulfate scale (bottom) [10].

Also recently new types of EDTA-based and have been introduced to industry that are more cost effective and cover larger types of scale like iron sulphate.

### 3.3.2 PREVENTING SCALE

Scale removing from a well is an expensive process and adding to the costs of deferred production which makes it even more expensive. To avoid this high costs, scale removal techniques, prevention methods are introduced to the industry. In most of the cases scale prevention through chemical inhibition is the preferred method of maintaining well productivity.

But chemical inhibition where chemicals are permanently injected into the production stream, is not the only way to prevent scaling.

There are numerous scale inhibitors introduced to oil industry. Main mechanism of these chemicals is blocking the growth of scale particles by poisoning the growth of scale nuclei. While a few of these chemicals chelate or tie up the reactants in a soluble form over a wider range, problems may occur if the inhibitors block and prevent crystals from growing only in a limited level of oversaturation.

Most of the scale inhibitors are phosphate compounds: inorganic polyphosphates, organic phosphate esters, organic phosphates, organic amino phosphates and organic polymers. These phosphate based chemicals generally minimize scale deposition by combination of crystal dispersion and scale stabilization Figure 14.

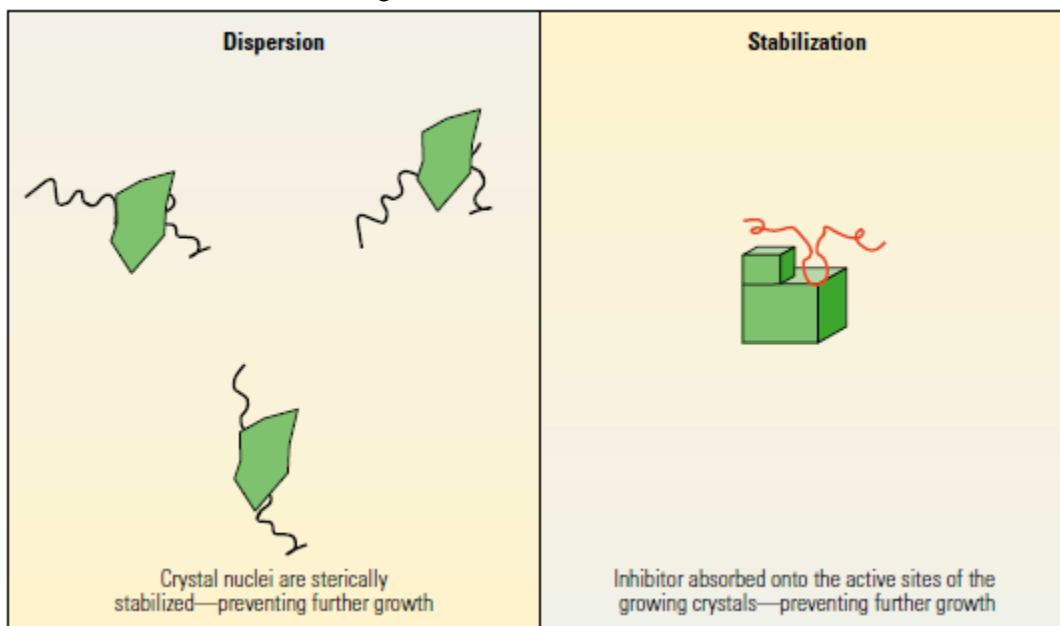


Figure 14 - Dispersion (on the left) prevent small seed crystals of scale from adhering to other crystal particles. Stabilization chemicals (on the right) modify the deposited scale structure, preventing additional crystal attachment [10].

Generally inhibitors are retained in the formation by either adsorbing to the pore walls or precipitating in the pore space. Treatment lifetime depends on surface chemistry, temperature and pH, which normally exceed one year for properly designed treatment. Long inhibitor lifetime could also be achieved by pumping large volumes of inhibitor such that the inhibitor is exposed to and absorbed to a large surface area.

In addition, there are some other methods to prevent and compensate scaling problem. Recent research demonstrates the effectiveness of utilizing coated grains in gravel packs by surface modification agent (SMA). SMA is a family of polymers that strongly adsorb to mineral surfaces, creating a hydrophobic film [17].

It has been reported that when ceramic gravels are coated with hydrophobic layer, permeability loss caused by scaling is minimized. In these tests non-coated ceramic gravels were compared with coated ceramic. Gravels were packed inside the cell and precipitation fluids were injected into the cell in high temperature environment. Increasing injection pressure was taken as measure for the scaling inside the non-coated gravel pack, however coated gravel pack does not show any pressure increment Figure 15.

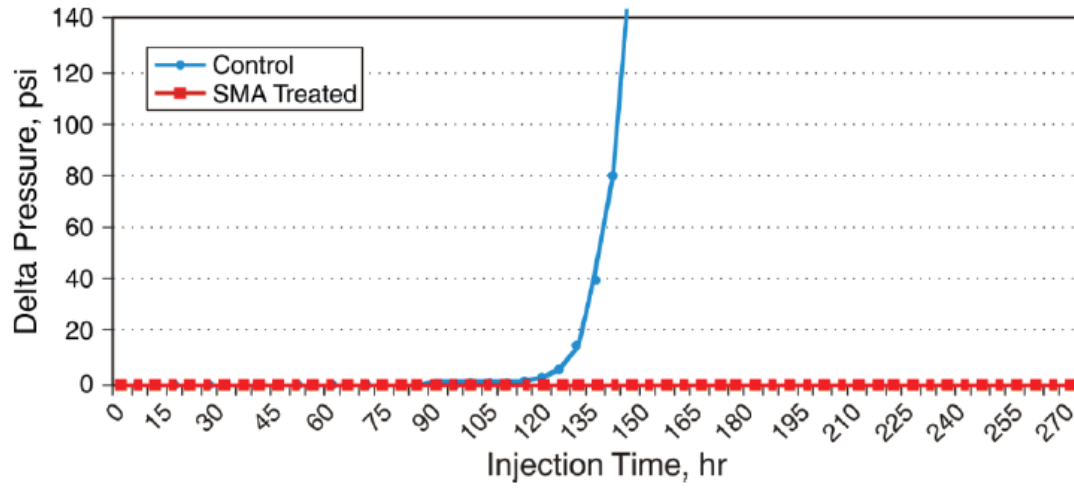


Figure 15 – The gravels treated with the water based SMA hydrophobic material shows no indication of plugging during the test period [17].

## 4 INNOVATIVE HYDROPHOBIC GLASS BEAD GRAVELS UTILIZATION TO CONTROL THE SCALING PROBLEM

### 4.1 INTRODUCTION

This chapter describes the experimental evaluation of the scaling tendency in non-coated and coated proppants made of glass and its comparison to ceramic proppant. As already explained in section 3.2 the reduction of permeability by scale in sand control installations is often resolved by removal of the acid soluble portions using organic or inorganic acids. These temporary solutions need work over operations and stop production for a certain time interval. To reduce or avoid these costs the idea of using self-scale inhibiting gravels by coating them with water repelling materials was looked at and technically evaluated.

As explained in the previous chapters, nucleation starts by creation of small crystal seeds. It was imagined that the hydrophobic film around the inert filter medium which apart of its water repelling characteristic makes the surface area extremely smooth and prevents the gravel surface from seeding the calcium carbonate scale formation. Secondly it was investigated if the assumption is correct that carbonates formed as homogeneous nuclei remain suspended and migrate through the pack.

In addition the excellent sorting and roundness of glass beads was deemed an advantage in the prohibition of scale deposit in gravel pack installations. This assumption is based on the observed increase of the effective pore space and therefore the permeability of the sand pack. In regards to scale deposit reduction it was thought that this permeability increment will help transporting of crystals easier through the pack leaving the individual nuclei less time for forming and adhesion to the proppant grains.

#### 4.1.1 HYDROPHOBICITY

Solid surfaces are defined in terms of hydrophilicity and hydrophobicity which describes the material ability to be water or non-water wet. The name of hydrophobic derives from Greek that is the phenomena of water repelling ability on the surface of material. Hydrophobic materials have non-polar surfaces thus they tend to wet with other non-polar solvents and not with the water.

Actually surfaces of materials and molecules consist of at least two parts. Soluble part called "lyophilic" and the insoluble part is called "lyophobic". As can be seen in the Figure 16, the hydrophilic part is referred to as the head group and the hydrophobic part as the tail.

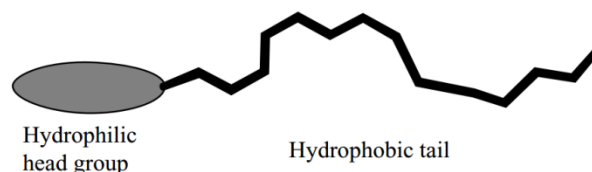


Figure 16 - Schematic illustration of a surfactant with hydrophobic and hydrophilic parts.

Additional factors that influence on the wetting behaviour consist of porosity, roughness, chemical heterogeneity or reactivity [18].

### Surface free energy and contact angle

Surface energy is defined as the work necessary to separate two surfaces beyond the range of the forces holding them together. It is defined in energy per unit area. Surface energy often referred to as surface tension and usually expressed in dynes/cm or mN/m (a surface tension of 1 dyne/cm or mN/m is equivalent to a surface free energy of 1 mj/m<sup>2</sup>). The surface energy for liquids often called surface tension, depends on the intermolecular forces within the material. A strong interaction between molecules gives a material with a high surface free energy and vice versa. For example water has a surface tension of 73[mN/m] due to its ability to form strong hydrogen bonds within itself.

The surface free energy of a solid can be indirectly estimated through contact angle measurements. Contact angles are closely related to wettability, the lower the contact angle the greater the wettability.

A liquid will wet a solid when its surface energy is lower than the solid's surface energy. Forced balance or equilibrium at solid liquid boundary is given by Young's equation for contact angles greater than zero (equation 12).

$$\gamma_{lv} \cos \theta = \gamma_{sv} - \gamma_{sl} \quad (12)$$

Where  $\theta$  is the contact angle, and  $\gamma_{lv}$ ,  $\gamma_{sv}$  and  $\gamma_{sl}$  are surface free energies of the liquid-vapour, solid-vapour and solid-liquid interfaces, respectively. The lower the contact angle, the greater the tendency for the liquid to wet the solid, until complete wetting occurs (contact angle  $\theta = 0$ ,  $\cos \theta = 1$ ). Large contact angles are associated with poor wettability.

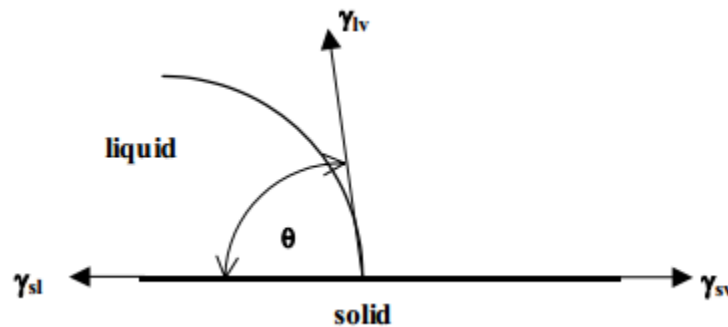


Figure 17 - Contact angle of a liquid on a surface

Contact angle is the angle between the liquid and the solid which appears when the solid is not completely wet, Figure 17. A low contact angle indicate a good wetting (hydrophilic surface) and vice versa.

The static contact angle alone is not sufficient when describing the hydrophobicity of a surface. In fact both increasing and decreasing the volume of drop (advancing and receding respectively) can effect on wetting condition. In this regards the sliding angle is defined, which is the angle needed for droplet of a specific size to start sliding down a tilted surface.

Equation 13 describes the force needed for a drop to start sliding over a solid surface. In this equation  $\alpha$  is the sliding angle,  $\gamma_{lv}$  is the surface tension of the liquid,  $\theta_R/\theta_A$  is the receding



respectively advancing angle,  $d$  and  $m$  are the diameter respectively the mass of the droplet and  $g$  is the gravitational acceleration (Chen et al. 1999), the parameters can be seen in equation 13.

$$F = \frac{mg \sin \alpha}{d} = \gamma_{lv}(\cos \theta_R - \cos \theta_A) \quad (13)$$

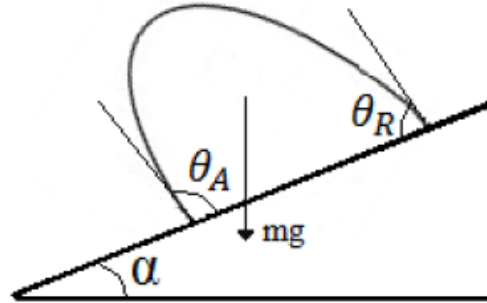


Figure 18 - An illustration of some of the parameters influencing the force needed for a drop to start sliding down a titled surface.

### Super hydrophobicity

A surface could be considered as super hydrophobic when it exhibits a contact angle above  $150^\circ$  and a low sliding angle generally there are two theoretical hypotheses to explain hydrophobicity in the micro structured surface. First one is Wenzel model which describes the wetting when the liquid fills the cavities of the surface, Figure 19, the idea in this model is the contact angle will increase due to the increasing surface area of roughened surface, compared to the smoother surface.



Figure 19 - The different wetting models (a) Wenzel and (b) Cassie-Baxter

The increase in contact angle can be described by equation 14 where  $\theta^*$  is the apparent static contact angle,  $\theta$  is the static contact angle if the surface would be ideally smooth and  $r$  is the ratio between the actual surface area and the projected surface area.

$$\cos \theta^* = r \cos \theta \quad (14)$$

The other theory is the Cassie-Baxter model that related to the case where air is trapped in the pockets underneath the liquid drop which is shown in Figure 19 (b). Here the rough surface

considered as a porous hydrophobic material which is unfavourable for the liquid to penetrate. This leads to entrapment of air, which can be considered as a hydrophobic phase, and thereby a higher exhibited contact angle of the liquid.

## 4.2 APPARENT PHYSICAL PROPERTIES OF SAMPLES

To approach the evaluation of hydrophobic coated glass beads, normal glass beads and hydrophobic coated ones are compared to each other. In addition to materialize a comprehensive evaluation, two other well-known gravels such as ceramic and natural quartz sands have been used. In the following sections, there is a detail evaluation on physical properties of selected material.

### Glass beads - coated and non-coated

All glass materials used in the following evaluation were provided by the SWARCO Company.

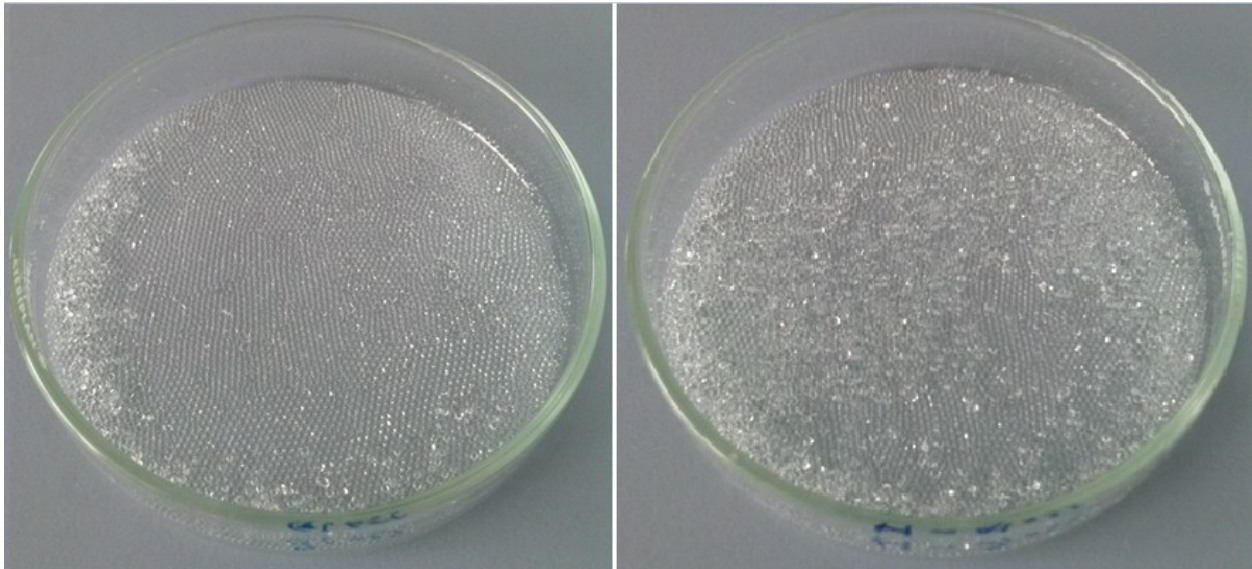


Figure 20 - Appearance of glass beads. On the right side hydrophobic coated glass beads and on the left side normal glass.

As it can be seen in Figure 20 the appearance of both coated and non-coated glass gravels are the same. Also they have the same absolute density of 2.51[gr/cm<sup>3</sup>].

Table 5 and Figure 21 show the particle size distribution measured with the Laser Diffraction method (LPSA) of the actual used material.

Table 5 - Gravel size analysis of glass beads with cumulative comparison in percentage

Unit metric(micrometer)	Cumulative. <	Diff.
	%	%
0	0.00	0.00
2	0.00	0.00
3	0.00	0.00
5	0.00	0.00
10	0.00	0.00

20	0.00	0.00
30	0.00	0.00
50	0.00	0.00
63	0.00	0.00
100	0.00	0.00
200	0.00	0.00
315	0.00	0.00
500	0.00	78.60
1000	78.60	21.40
2000	100.00	0.00

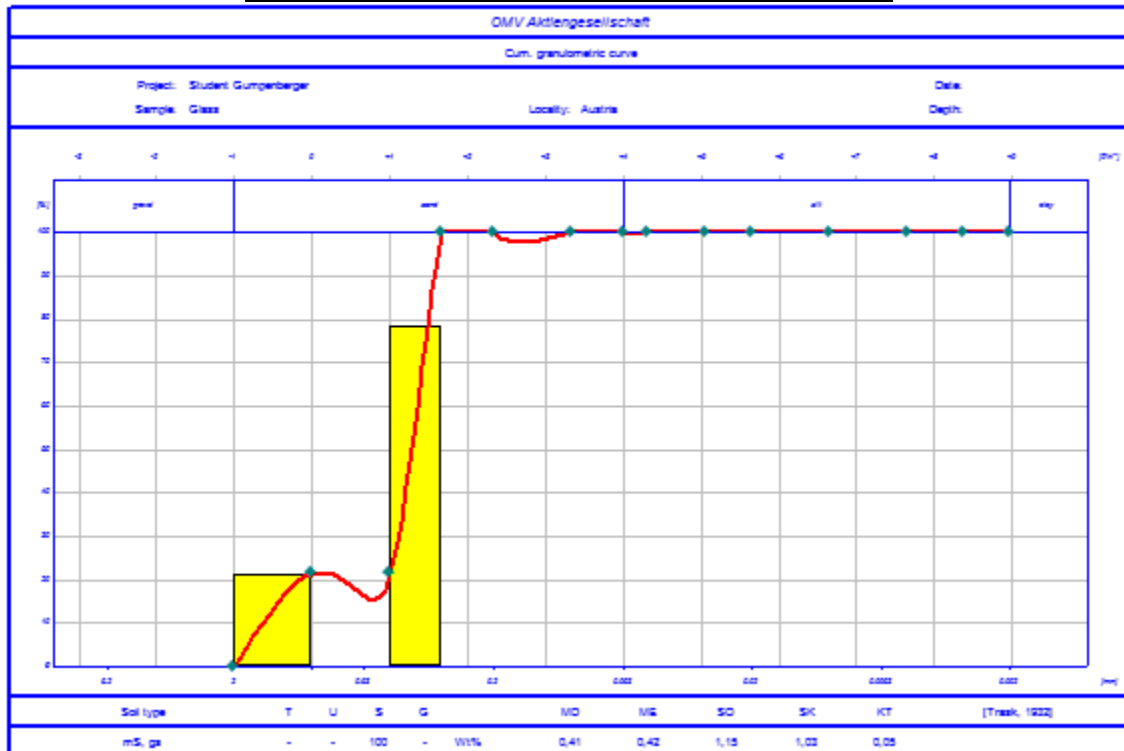


Figure 21- The cumulative size analysis of glass beads by phi number on the top and mm at the lower axis at bottom.

The particle size distribution of the glass proppant material shows that 78.6% of grains are between 500 and 1000 micrometer. Based on measurements using the microscope, the average diameter of each grain is around 950 micrometer.

Since the LPSA grain distribution represents a very narrow range, the reference grain size was determined by the average diameter of some grain sizes measured via microscopic pictures. Figure 22 and Figure 23 show the coated and non-coated glass beads. Measurements based on these pictures give the average diameter of 950 micrometer for glass beads.

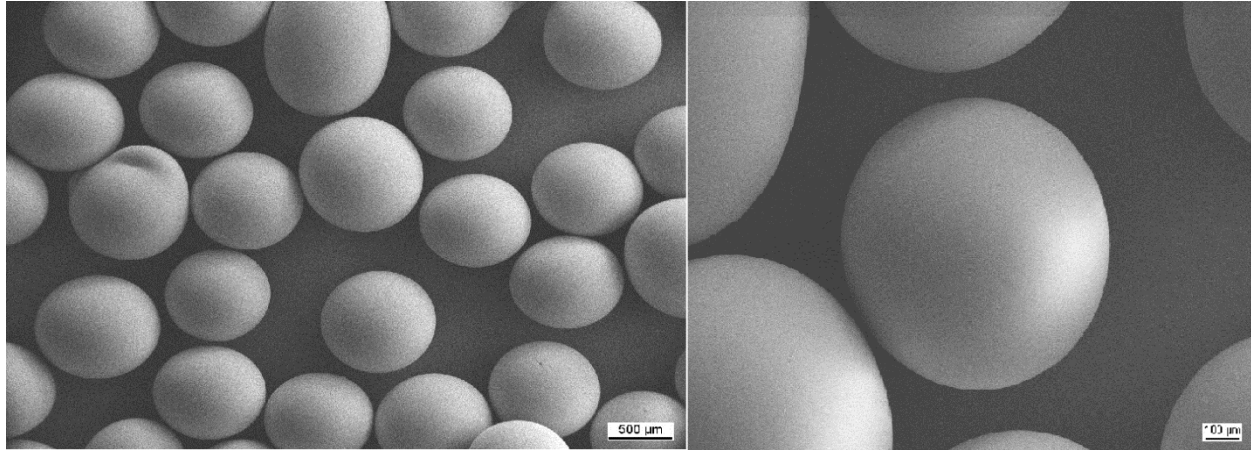


Figure 22 - Microscopic pictures of normal non-coated glass beads.

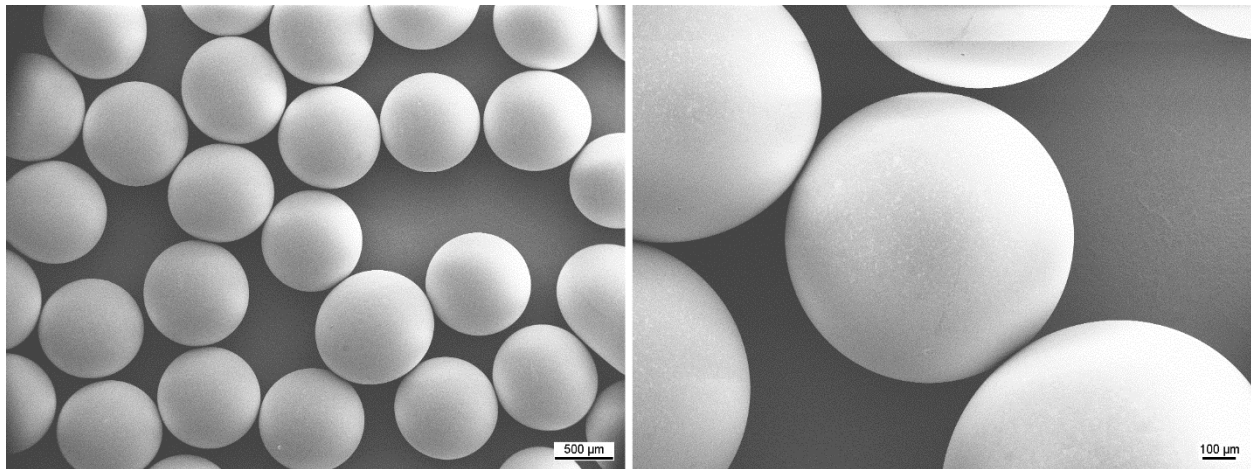


Figure 23 - Microscopic pictures of hydrophobic coated glass beads.

Although normal and coated glass beads are the same in size, density and appearance, they show completely different behaviour in contact with water. Figure 24 compares the hydrophobicity effect between normal and hydrophobic coated glass. 2 cc water was added on a surface covered by glass beads. On the surface of non-coated proppants, since it is water wet, the water distributed uniformly everywhere over the glass beads.

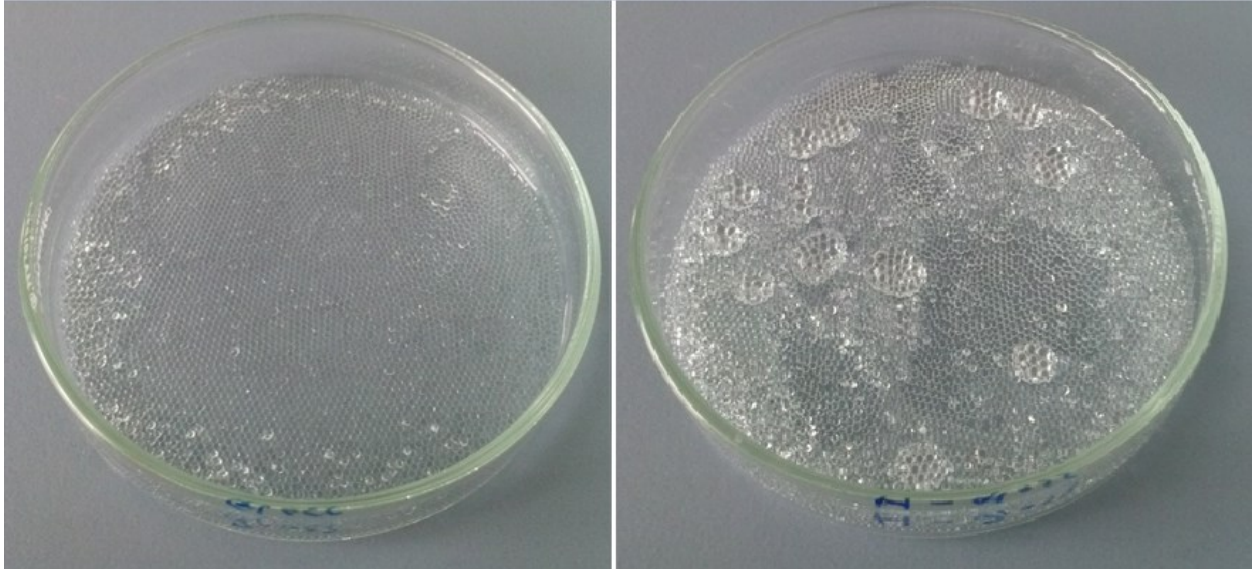


Figure 24 - 2 cc of distilled water is added to both types of glass beads. On the left side normal glass and on the right side hydrophobic glass

By adding water to the surface of hydrophobic glass beads, water droplets formed. Water did not absorb to the grains or entered the pore spaces. Figure 25 demonstrates the contact angle of water on the surface of hydrophobic glass beads, for one water droplet.

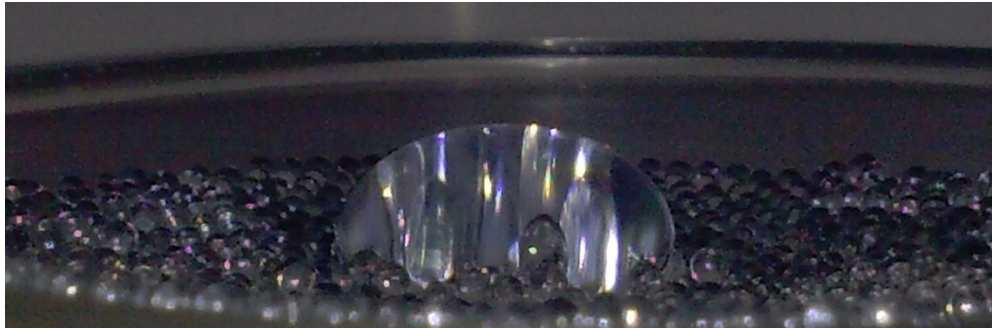


Figure 25 - One droplet of water on the surface of hydrophobic glass beads.

### **Ceramic and natural quartz sand**

Ceramic gravels and natural quartz sands are both used in the petroleum industry in gravel packing systems for many years. Quartz sand is a natural material that contains mostly quartz and some other compositions. Figure 26 (left picture) shows the apparent picture of sand gravels in 20/40 mesh size that have been used in the laboratory tests. The other photo also shows the ceramic gravels with mesh size 20-40.

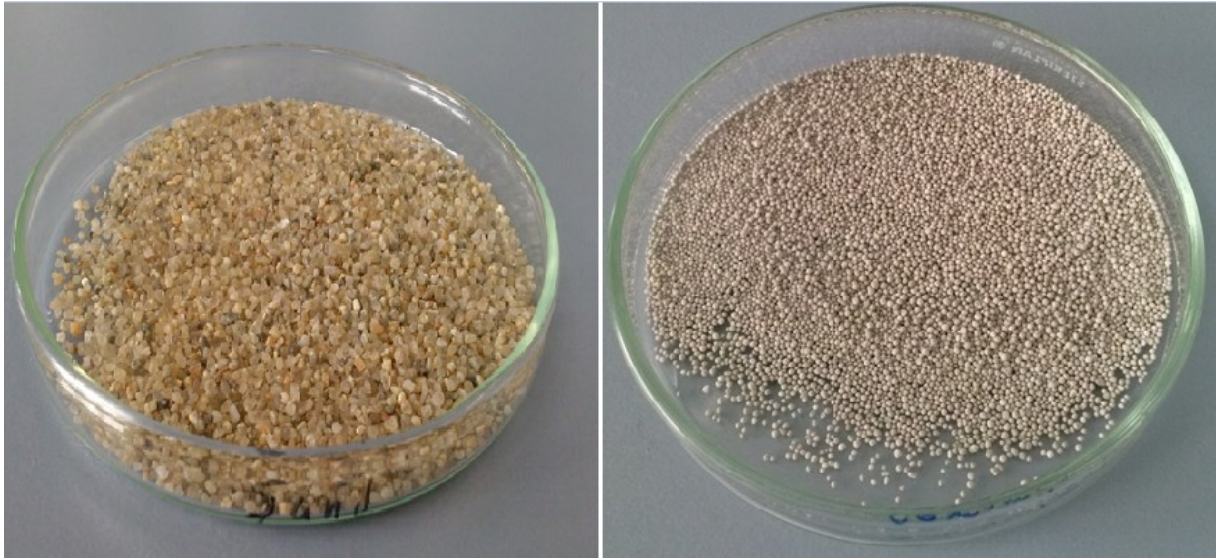


Figure 26 - On the left side natural quartz sand and on the right side ceramic proppant.

Density of ceramic and natural quartz sand are respectively, 2.66 and 2.65 [gr/cm<sup>3</sup>].

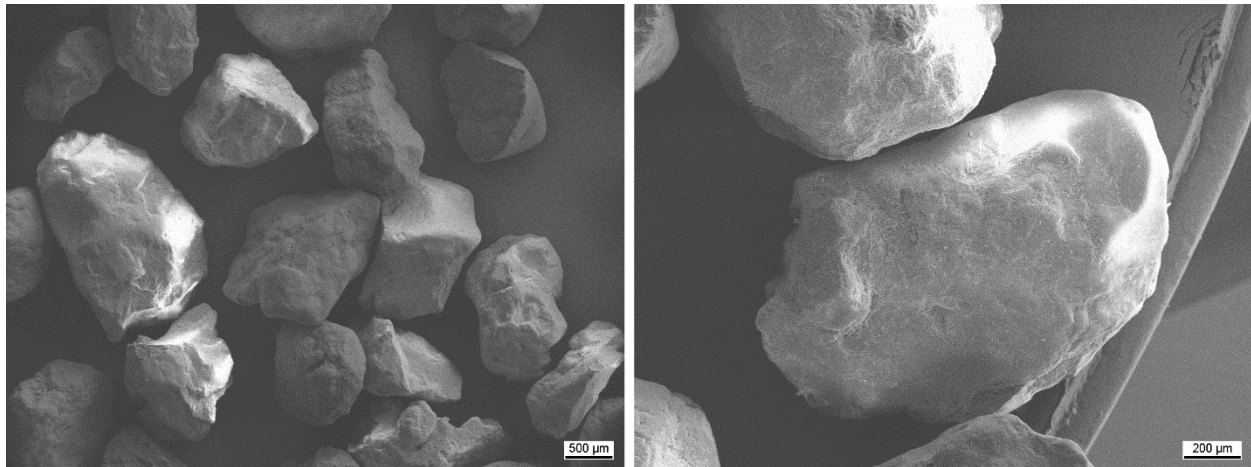


Figure 27 - Normal quartz sand microscopic picture.

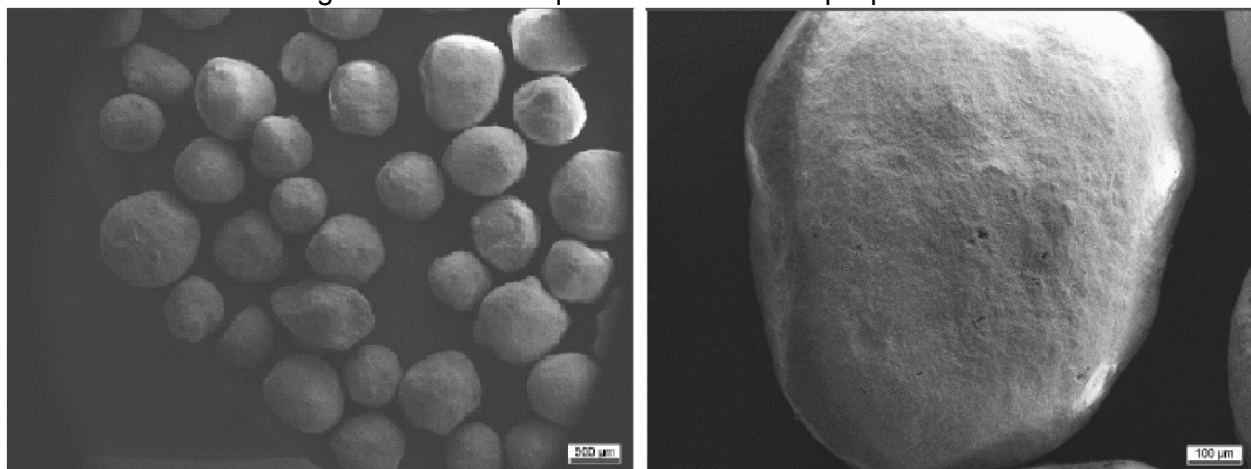


Figure 28 - Ceramic grains microscopic pictures.

Figure 27 and Figure 28 represents size and shape characteristics of natural quartz sand and ceramic proppant. Based on this microscopic measurements average diameter of ceramic and quartz sand are respectively 1 mm and 1.7 mm, which shows that sand grains are significantly larger than ceramic. Also ceramic has higher sphericity in comparison with quartz sands (sphericity definition in Appendix B).

Since the available quartz sand consisted of some other compositions that can be seen in Table 6 , was not very well sorted and contained fine material, the natural sand was not used for comparison with the glass beads in the precipitation tests. On the other hand, the ceramic proppants which are artificially manufactured like glass material, demonstrated comparable sphericity and sorting of the particles. Because of the better comparability of the ceramic and glass proppants only these two materials were used for permeability and precipitation tests.

Table 6 - Composition analysis of normal quartz sand grains

Quartz	K-Fsp	Plag	Calcite	Dolomite	Ankerite	Siderite	Anhydrite	Fluorite	Pyrite	Clay Tot+Mica
88.2	8.7	1.4	-	1.7	-	-	-	-	-	-

### Gravels aggregation in water

Tackiness causes gravels aggregation, resulting in reduced gravel-pack densities (increased porosity and permeability). As can be seen in Figure 29, water was added to the same volume of all gravel types and hydrophobic coated demonstrated more volume increment in comparison to others. The reason is that water does not penetrate easily into pore space of hydrophobic coated glass beads. That's why after adding water a mixture of air and water create in the pore throats and existence of air in between proppants reduce the weight of them and increase the buoyancy of the grains in the water.

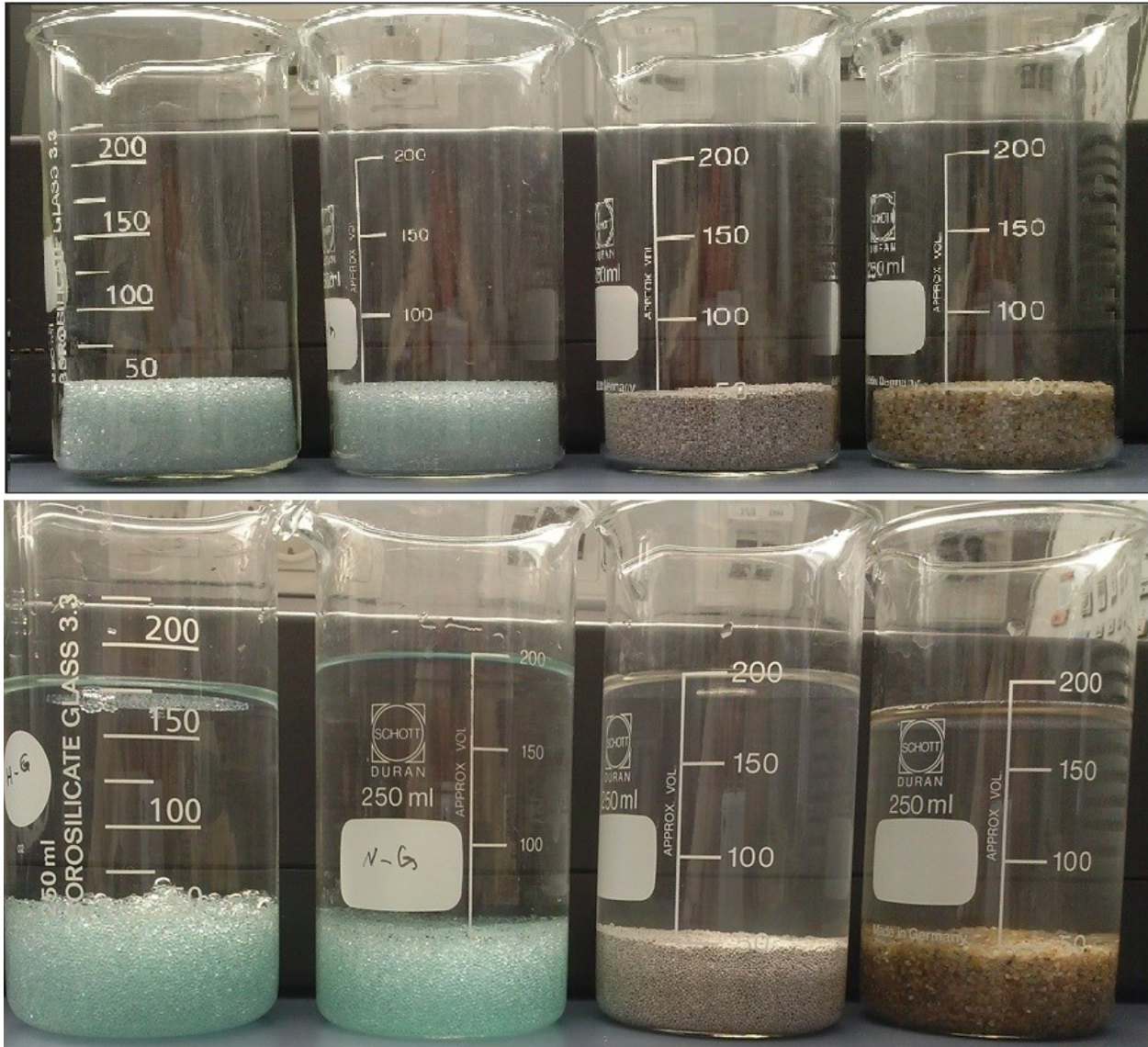


Figure 29- dry samples (on the top) and samples after adding water (down).

### 4.2.1 TOOLS AND EQUIPMENTS

The used tools and equipment in the laboratory tests are consists of:



Pump: two pumps were used for the whole experiment, one centrifugal pump to determine the base permeability, because of pulsation in reciprocating pumps. Another pump to inject the mixture into the cell for precipitation. Because injection of precipitation fluid need to be done in a very low and exact rate to give time to fluid to adhere on grain`s surface. In this regards the pumps were used in this experiment are:

1. The LC-20AT possesses a high level of stability while maintaining high performance during routine use. The ability to remove pulsations has been improved by modifying the pump-head structure and the flow line. Usage of this pump makes it possible to provide exact flow rates. In precipitation tests it is necessary to have two pumps with exactly the same flow rate of 2 [ml/min] for each one.
2. GRUNDFOS-TP-Vertical: it`s a centrifugal pump, so gives a good pressure drop in the system with low fluctuation. The highest flow rate with this pump is 23 ml/sec.



Figure 30 - The centrifugal pump (GRUNDFOS-TP-Vertical) on the right side and reciprocation pump (LC-20AT) on the left

Oven: Memmert UFE 500

That UFE stand for, U is Universal, F is forced air circulation fan and E means excellent (Figure 31). The oven was used for heating process at scaling tests. Since thermal energy makes the chemical reaction possible in precipitation tests. The gravel packed cell was placed into the heater.



Figure 31 - Memmert UFE 500

- Steel Cell: 20 centimetre length and 5 centimetre diameter (Figure 32). This contains: Outlet filter, Inlet filter, Inlet end piece with O-ring, Outlet end piece with O-ring, but there were some problem with this system. First one was the low pressure drop, because the amplifier was always (with all different rates) showing a pressure drop of less than 0.01, and second the large cell makes it difficult to pack the gravels properly and as a result with different packing condition and by small changes in pressure the permeability changing was significant.

To have the higher pressure drop (for easier and more reliable analysis) and more uniform packing condition, reducing the diameter of the cell to around 1 cm seems a good idea (Figure 33).

In addition during the scaling tests, it was easier to demonstrate increment in the pressure difference or decreasing the permeability in the cell with smaller diameter. Because in the larger cell, the differences are small and difficult to recognize and analys.

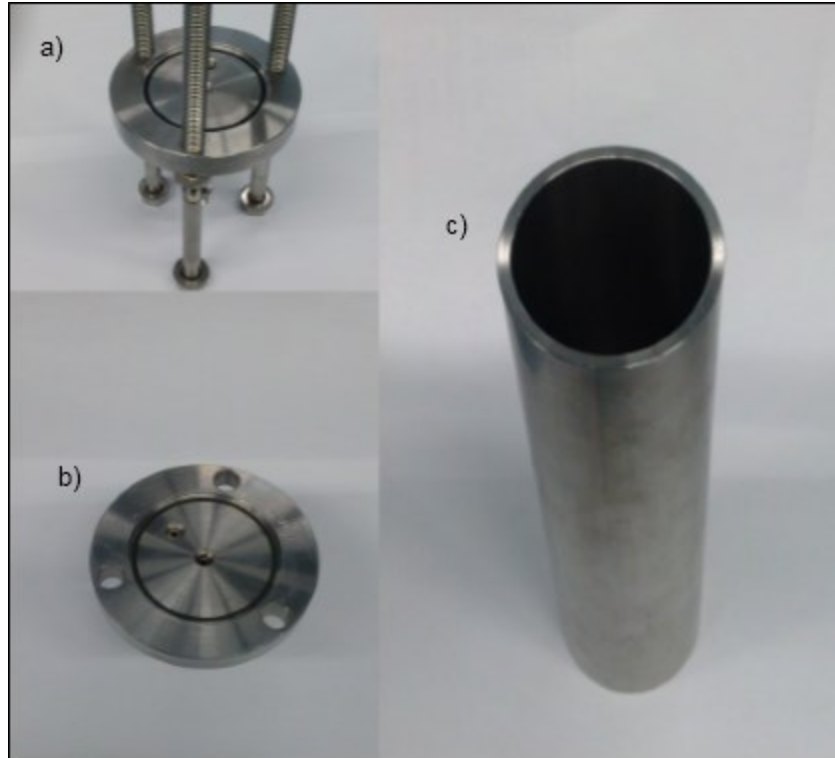


Figure 32 - the steel cell. a and b respectively shows the inlet and outlet end and c is the 20 cm length steel cell



Figure 33 - second steel cell with 1.18 cm diameter. a,b)inlet or outlet connection to cell with sieve d,f)inlet or outlet connection from pump c,e)connection to pressure transducer g)the cell

- Amplifier: MGC plus that using it for data acquisition with its supporting transducers, fieldbus connections and computer analysing software's.



Figure 34 - MGCplus amplifier

- Scale: OHAUS explorer pro 1ft gold scale (Figure 34). The maximum weight capacity is 41 grams and is capable to connect to computer for analysis. The flowing rate was calculating from output fluid from cell that was weighting by scale.



Figure 35 - Scale - OHAUS EXPLORER

## 4.3 PERMEABILITY EVALUATION WITH BASE FLUID

### 4.3.1 PERMEABILITY

The permeability of a medium is an expression of the medium's fluid transmission capacity and can be considered as a reverse of the medium's resistivity to an internal flow of fluids. Only single phase (water) permeability is considered in this thesis.

In order to calculate the absolute permeability the medium must be 100% saturated. In this case the absolute permeability is measured by injection of water through a filter medium in a cylinder fully packed with gravel. When measuring the flow rate,  $q$ , of a single phase fluid versus the pressure difference, Darcy's equation allows to determine the permeability of the medium:

$$\text{Darcy equation} \quad q = \frac{KA \Delta P}{\mu L} \quad (15)$$

Where

$q$  is fluid flow rate [ $\text{m}^3/\text{s}$ ]

$\Delta P$  is the pressure difference [Pa]

$\mu$  is the viscosity [Pa.S]

$L$  is length [m]

$A$  is cell cross section [ $\text{m}^2$ ]

Based on units defined above, permeability will calculate in [ $\text{m}^2$ ] which is  $10^{12}$  Darcy ( $1\text{m}^2=10^{12}\text{D}$ ).

### 4.3.2 PROCESS AND TEST SETUP \_ BASE PERMEABILITY

The test setup is designed to use the Darcy equation for permeability determination. Water at a specific flow rate was forced through the pore space of the gravel pack system and the pressure difference in inlet and outlet was measured. The measured values were evaluated, using Darcy equation to calculate the permeability of the pack.

As it can be seen in Figure 36 the water pump from a container through the gravel pack cell. The inlet and outlet pressure was measured by transducers and recorded by computer. The outlet water was recouped in a container placed on the scale and measure the outlet weight. Since density of water is 1 [gr/ml], changing in the weight over time [sec] results, water flow rate [ml/sec]. Therefore according to equation 16 the amount of injected water is calculate by ml:

$$\frac{(\text{changes in weight on the scale})[\text{gr}]}{\text{water density}[\frac{\text{gr}}{\text{ml}}]} = [\text{ml}] \quad (16)$$

Dividing the injected volume by time interval results flow rate [ml/s]. Also both scale and amplifier are connected to computer to calculate and record the changes versus time.

To find the absolute permeability of gravel packs simple equation of Darcy is used, equation 17:

$$k[\text{m}^2] = \frac{Q[\text{m}^3/\text{s}] \times \mu[\text{pa.s}] \times \Delta L[\text{m}]}{\Delta P[\text{pa}] \times A[\text{m}^2]} \quad (17)$$

The whole process is shown in Figure 36.

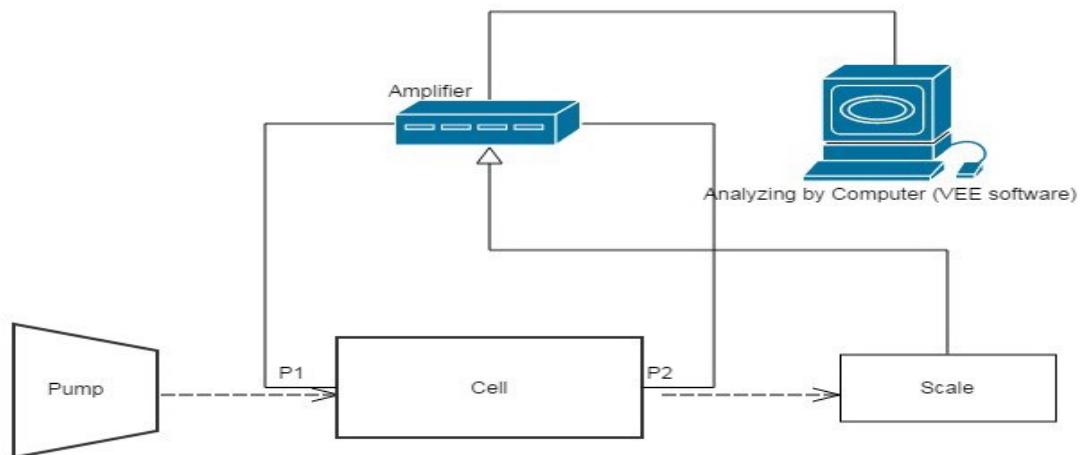


Figure 36 – Setup to measure permeability. P1 and P2 refer to inlet and outlet pressure respectively

### 4.3.3 TOOLS AND EQUIPMENT \_ BASE PERMEABILITY

The following equipment were used to measure the base permeability:

- Gravel packing cell, Figure 33
- Pump, Figure 30 (centrifugal pump)
- Scale, Figure 35
- VEE Software
- Amplifier and pressure transducers, Figure 34
- Tubes to connect pump, cell and scale

### 4.3.4 TESTS AND RESULTS

The following outlines detailed instruction of packing, soaking and water injecting into the gravel pack is explained in the following:

- Install and fix the sieve in the inlet lid, on one side of the cylinder.
- Pure gravels into the cylinder and compact it to make a good packing.
- Install a sieve inside the outlet lid and place it on the other side of the flow tube.
- Connect the cylinder to the pump and put it in a vertical position.
- Pump water from bottom of the cell to top to soak the grains for 5 minutes.
- Connect pressure transducers at the top and bottom outlet.
- Fix the gravel packing cell above a container of which the weight can be measured by the scale in the vertical position and start pumping from top to bottom. Measure the pressure difference between inlet and outlet and weight of pumped volume to calculate flow rate and permeability.

Corresponding the explanation in the previous section, permeability could be calculated simply by having flow rate and pressure drop. To achieve these two variables, a system provided (Figure 36) that contains a pump with constant flow rate and a cell with 24 cm length and 1.18

cm diameter to pack gravels in it, and two pressure transducers to measure the pressure at inlet and outlet.

Since ceramic and natural quartz sands are usually used by oil companies they were considered as a base criterion for comparison with glass beads.

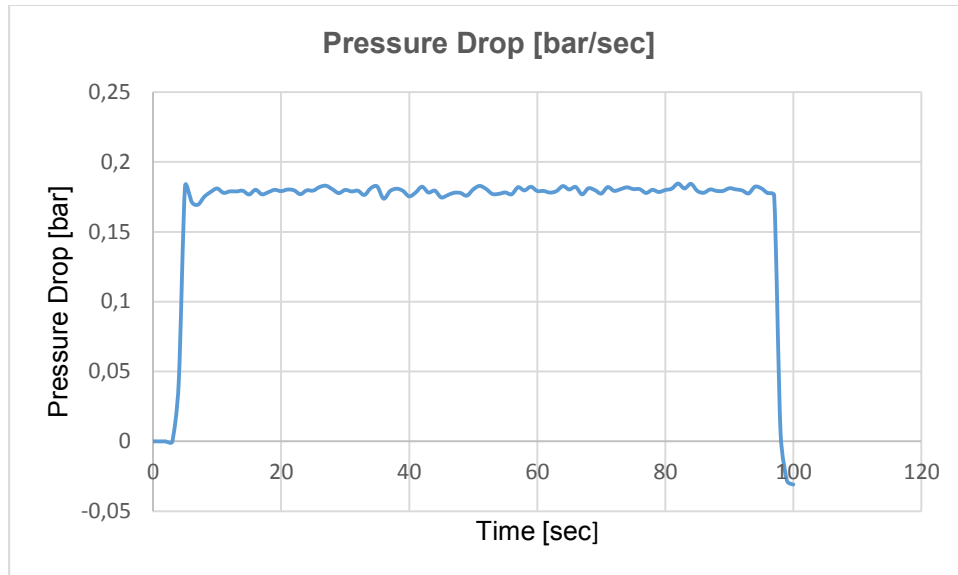


Figure 37 - Pressure drop in ceramic permeability test

Throughout several tests on ceramic gravels by flow rate of 1.44[ml/s], the permeability calculated is around 200 Darcy. Slightly changes in permeability are because of fluctuation in flow rate or pressure that comes from pump and transducer operating modes. The pressure drop and rate can be seen in the Figure 37.

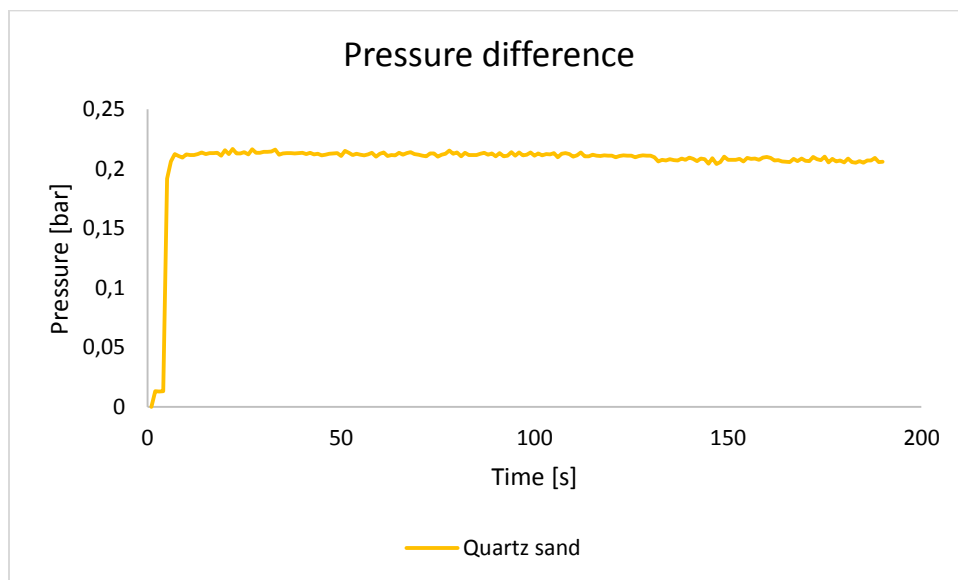


Figure 38 - Pressure drop of quartz gravel sands.

With the same process the permeability of other samples is calculated. With the same flow rate of 3.1 ml/s, the pressure drop in hydrophobic and normal glass beads are the same (400 Darcy) as can be seen in the graph, Figure 39.

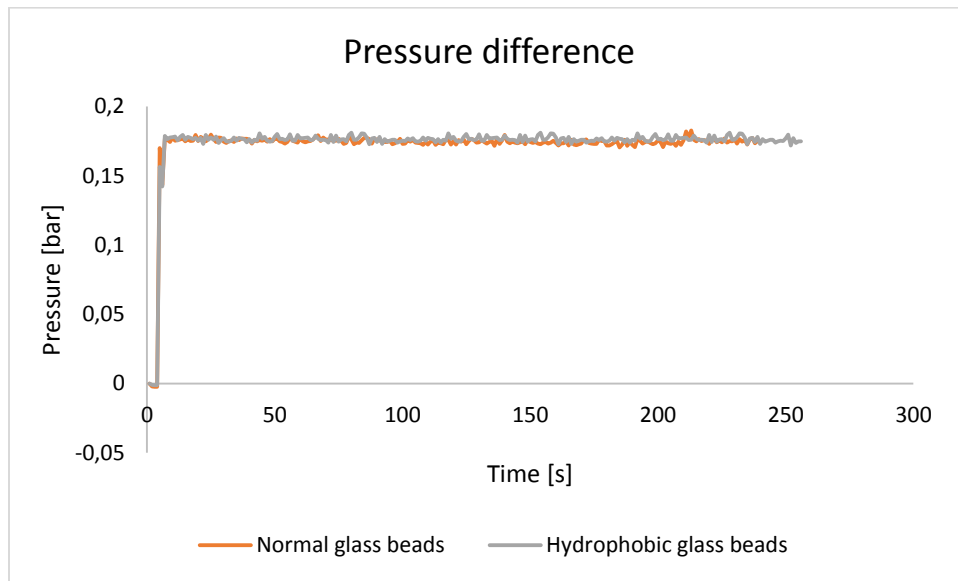


Figure 39 - Pressure drop through both hydrophobic coated and normal glass beads are the same.

was seen (Figure 38). The poor coated sand even with larger grain sizes resulted in lower permeability.

#### 4.3.5 DISCUSSION

As can be seen in Figure 40, both coated and non – coated glass beads have the same permeability.

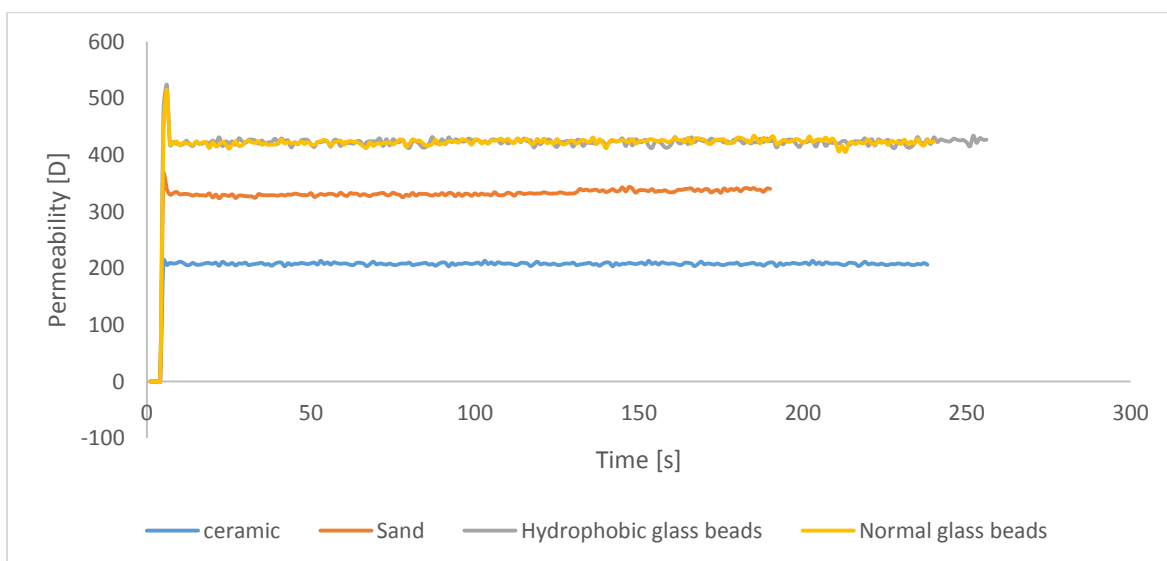


Figure 40 - Compare permeability of different samples.



This results confirm that permeability in this gravel pack system is just related to the following factors:

- Pore size and grain size
- Grain size distribution
- Shape of grains
- Packing of grains

Glass beads have the highest permeability in comparison to the other samples. Although ceramics (with 1 mm grains diameter) are in the same size with glass beads (with 950 micro meter diameter), because of better sorting and sphericity, glass beads are more permeable.

On the other hand sand grains with 1.7 mm diameter are almost two times larger than other samples, but because of bad sorting and very low sphericity they have 100 Darcy lower permeability than glass beads.

Due to larger size of quartz sand material, to have a better comparison, glass beads and ceramic which have the same size were compared in Figure 41 and quartz sand is not considered in this comparison.

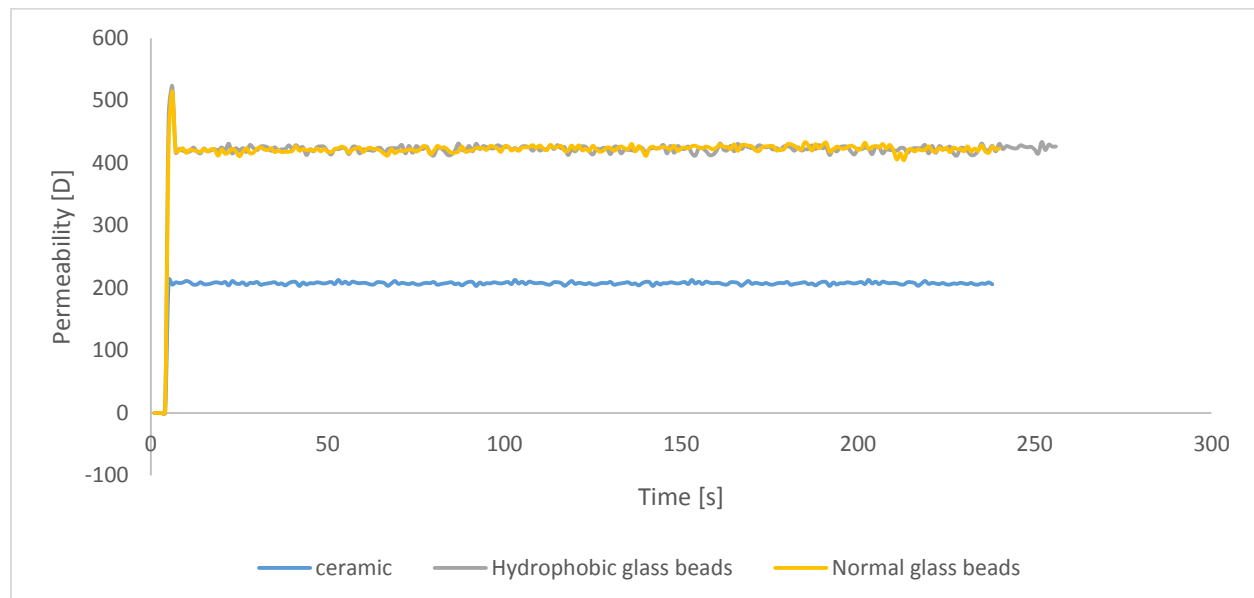


Figure 41 - Permeability collation of glass beads with ceramic.

Another important point that need to be considered is the pump power which was the same for all the tests, while the flow rates were calculated by scale is different between ceramic and glass. The flow rate in glass gravel packing is more than in ceramic and the reason is that the different pressure drop and energy are needed to push the water along the glass pack in compare to ceramic pack. The same energy is given to pump, but the pore space in glass packing is more, therefore to have the same flow rate in ceramic pack with less pore space, the more energy need to be given to the pump.

The slight fluctuations in permeability shown in Figure 40, is related to pump parameters and pressure transduce accuracy.

To calculate the effect of utilization of the glass beads in the bottom hole condition, both ceramic proppants and glass beads were considered in the same pressure drop with the known

permeability of 400 D for glass beads and 200 D for ceramic. Equation 18 shows the bottom hole condition radial flow regime, that in the same pressure drop at radial condition glass bead gravel pack represent two times higher flow rate than ceramic gravel pack.

$$\Delta p = \frac{q\mu}{2\pi hk} \left( \ln \frac{r_t}{r_w} \right) \quad (18)$$

$$\frac{q_{\text{glass bead}}}{q_{\text{ceramic}}} = \frac{k_{\text{glass bead}}}{k_{\text{ceramic}}} = 2 \quad (19)$$

where

$q_{\text{glass bead}}$  is flow rate in glass bead gravel pack system

$q_{\text{ceramic}}$  is flow rate in ceramic gravel pack system

$k_{\text{glass bead}}$  is permeability in glass bead gravel pack system

$k_{\text{ceramic}}$  is permeability in ceramic gravel pack system

$\Delta P$  pressure drop

$r_t$  is tubing radius

$r_w$  is well bore radius

## 4.4 PRECIPITATION TESTS

### 4.4.1 LABORATORY EXPERIMENTS FOR PRECIPITATION OF CALCIUM CARBONATE (PCC)

Due to industrial applications and market demands, precipitation of calcium carbonate (PCC) has received significant attention in recent years. Generally in the industry two types of natural (limestone, marble, chalk and coral) and synthetic (precipitated) calcium carbonate are used. The natural calcium carbonate comes from mineral processing to meet the quality.

The precipitated calcium carbonate can be synthesized via solution (liquid-liquid-solid) or by carbonation (gas-liquid-solid). The first route regarding the easiness in controlling the process variables, is often adopted by laboratory experiments.

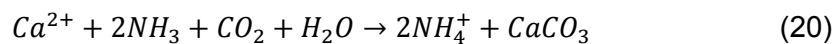
The liquid-liquid-solid method is usually done by combination of two fluids that are rich with different ions.

The carbonate synthesis is used in the industry, due to the availability of raw materials and their low costs. The procedure consists of bubbling  $\text{CO}_2$  gas through an aqueous  $\text{Ca(OH)}_2$  suspension in a batch reactor [19, p. 2].

Here there is a brief explanation about these two artificial approaches for generation of calcium carbonate.

#### Gas-Liquid-Solid

Calcium carbonate precipitates by injecting  $\text{CO}_2$  gas to solution with  $\text{Ca}^{2+}$ . Usually to have the calcium ion in the liquid solution, suspension of  $\text{Ca(OH)}_2$  is added to solution. Equation 20 shows the reaction:



### Liquid-Liquid-Solid

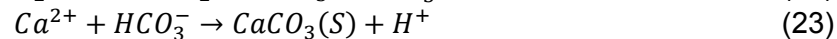
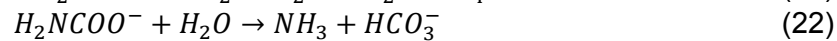
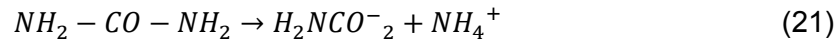
**Davor Zadovic et al** [20], introduced a dynamic technique to measure calcium carbonate scaling in a capillary stainless steel. The objective in this experiment is to measure the effect of inhibitor agents on scaling rate.

In this method two fluids containing bicarbonate (fluid A) and calcium (fluid B) were injected in the tubing. Also since chemical reaction need energy, the tubing is placed in the heater.

Pressure increment shows the tube is blocking with scaling fluid. With concentration of 1.68 g/l of solution A and 1.764 g/l of solution B the scaling observed after 8 to 12 minutes and full blocking occurred after 20 to 24 minutes.

**Fleming N et al.** (2011), introduced another method for precipitation of calcium carbonate, the objective of this method was downhole consolidation by chemical reactions to form in-situ calcium carbonate precipitation.

The technology is called Quasi-natural consolidation (QNC) which involves squeezing into near wellbore predefined concentrations of urea and calcium bicarbonate along with the enzyme urease. As can be seen in the chemical equations the Urease react with water and  $\text{HCO}_3^-$  is the outcome that react with  $\text{Ca}^{2+}$  and result calcium carbonate [21].



The sand pack put into the cell and the solution injected at 30 ml/min for 5 minutes and afterward the cell was closed and placed in the oven at 50°C for 24 hours.

### 4.4.2 PREPARATION OF THE PRECIPITATION PROCESS

Corresponding to laboratory limitations, choosing a feasible process, defining variables and effective factors are necessary before the setup for evaluating the scaling tendency in gravel packing porous media is designed.

In the first step the more feasible and easier method for creating scale in the laboratory was chosen. Second, it was decided that the setup has to be dynamic for a better representation of the bottom hole conditions. Third is the speed of reaction, it has to be logical and feasible to apply it in the laboratory. While in real field conditions scaling in gravel packing occurs after some years, in laboratory a very short process need to be designed (in some days or hours). On the other hand, the time interval has to be long enough for precipitated material to adhere on the surface of grains, so the chemical reaction should not be too fast (like in some seconds).

First and simplest idea to have precipitation and adherence of calcium carbonate on grain's surface, is to flow an oversaturated solution of calcium carbonate in water to the gravel pack cell and increase the temperature. But due to the low solubility of calcium carbonate in water (0.0013 g/100 mL at 25°C) this method would not give satisfactory results.

As explained in section 4.4.1, there are two common systems to create precipitation of calcium carbonate. First approach is with the mixture of gas and fluid, but this is a difficult technique due to laboratory limitations. The other system which is more preferable in this laboratory project consist of mixing two different fluids.

To use the Fluid-Fluid-Solid method, chemical compositions and concentration of each one need to be defined. Since the Fleming's technique is not dynamic, it is not a desirable method.

The other method (Davor Zadovic et al) is based on the dynamic injection of the mixture of sodium nitrate (fluid A) and calcium chloride (fluid B) into the sand pack. This system is easier to realize in regards to time interval and feasibility in laboratory.

To define the best concentration of sodium bicarbonate and calcium chloride in the fluids to mix. Five different concentrations of fluid A and B were mixed. Solutions with 1, 2, 3, 4 and 5 [gr/lit] sodium nitrate (fluid A), and 1, 2, 3, 4 and 5 [gr/lit] of calcium carbonate (fluid B) were mixed at equal concentrations. For example 50 ml, concentration of 1 [gr/lit] of fluid A was mixed with 50 ml of 1[gr/lit] fluid B, Figure 42.

Note: When the concentration of sodium nitrate and calcium carbonate was greater than 2 grams per liter, the amount of colloidal particles increased and the solution immediately became turbid, while in solution below this concentration the resulting fluid was transparent.

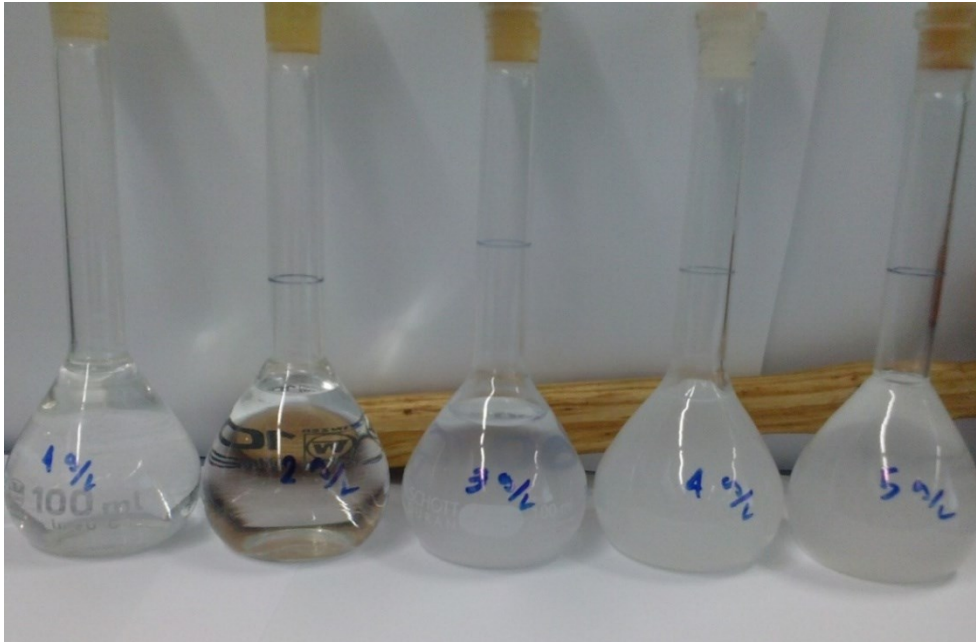


Figure 42 - 50% mixture of fluid A and B in concentrations of 1, 2, 3, 4 and 5 [gr/lit] respectively from left to right. The photo represent the condition of mixtures after 5 minutes from mixing.

As already discussed in section 3.2.1, chemical reactions between two fluids require thermal energy. Thus the samples were heated in the oven for 30 minutes to reach 80°C. Figure 43 shows the samples after heating. The bubbles in the sample with concentration of 1[gr/lit] are Carbon dioxide, which is the sign of reaction between two fluids (fluid A and B). Incrementing the concentration to 2 [gr/lit] the number of bubbles increased. While concentrations of 3 up to 5 [g/l] Calcium carbonate was already formed and precipitated.

From this test results using different concentrations it was deduced that mixtures with concentrations more than 2 [gr/lit] start nucleation too fast that is not suitable for testing. The colloids in the fluid meant that the radius of crystals get large enough to continue the reaction without thermal energy requirement, because of negative free energy. Therefore when the particles radius exceed a limit then enlargement of crystals is not anymore restricted by free energy and all soluble materials in the mixture will react with each other even without additional thermal energy provided by the oven (for more information see Appendix A).

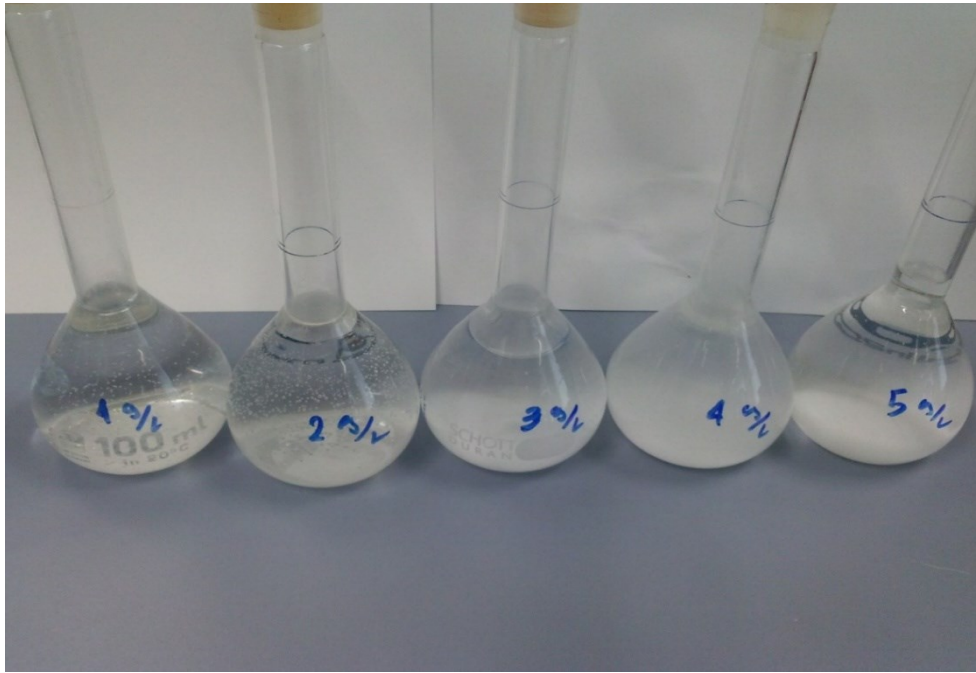


Figure 43 - Samples after 30 minutes heating at 80°C.

Based on these results, to have precipitation of calcium carbonate by reaction of sodium bicarbonate and calcium chloride in high concentrations, very little thermal energy is needed. While in low concentrations a significant thermal energy is needed.

Another important factor that impacts the reaction and results calcium carbonate precipitation is increasing pH. To evaluate the effect of pH a transparent mixture with concentration less than 2 [gr/l] of fluid A and B was mixed.

Based on molecular weight in the reaction (equation 24), to precipitate 1 gr of calcium carbonate 1.68 [gr/lit] of sodium bicarbonate and 1.47 gr of calcium chloride was mixed.



Then a mixture of 4[gr/lit] of NaOH in water was provided as a high pH fluid. After adding 2 cc of high pH mixture of NaOH precipitation start very fast as can be seen in Figure 44 a white suspended material in the mixture is gradually settling down.



Figure 44 - Increasing pH in the mixture of 1.68 gr/l sodium bicarbonate and 1.47g/l of calcium chloride. First picture from left side is fresh mixture and in each step 1 cc of NaOH mixture is added. By increasing pH the amount of white suspended material which  
 Since precipitation with increasing pH is very fast and does not simulate the condition in down hole this method was not considered for testing procedure.

#### **4.4.3 PRECIPITATION OF CALCIUM CARBONATE IN GRAVEL PACKS-DYNAMIC TESTS**

The objective of this section is to introduce a proper setup that represents the scaling tendency in hydrophobic gravel packing system and compare it with other non-coated types. It is expected that hydrophobic layers would not let the inorganic water soluble material adhere on the glass proppant. Thus tests had to be designed to provide the right conditions for calcium carbonate scales to allow them to adhere on the surface of gravels and ceramic proppants to make it possible to compare and evaluate the idea that this mechanism will not occur in the innovative glass material.

Corresponding to the concentration test that have been done in previous section (4.4) and discussion about nucleation and generation of clusters in the previous chapters and Appendix A, to design a dynamic setup, precipitation of calcium carbonate in gravel packs was tested based on two different ideas. First was scaling in atmospheric condition and without increasing temperature, and second one was with temperature in lower concentration.

##### **4.4.3.1 PRECIPITATION IN ATMOSPHERIC CONDITION-DYNAMIC SETUP**

Based on concentration tests in section 4.4.2, by increasing the fluid's concentrations more than 3 [gr/lit], precipitation occurs at room temperature.

In the designed setup, fluid A (solution of sodium bicarbonate) and B (solution of calcium chloride) were pumped separately into a chamber where they were thoroughly mixed before injection into the gravel pack cell (Figure 45). Both fluids were pumped separately with the same rate of 2 [ml/min] into the mixing chamber. During the pumping, the pressure transducer in the inlet of the cell records the pressure value (in bar). Any increment in pressure was interpreted as a result of plugging of gravel pack by calcium carbonate precipitation. The grade of precipitation, could be easily demonstrated by pressure increments. Also the injection rate was measured by the weight of the effluent, similar to the previous procedure for determining the permeability. The cell have been used in this test had 1.118 cm diameter and 24cm length and the concentration of mixture was 4 [gr/lit] for each fluid.

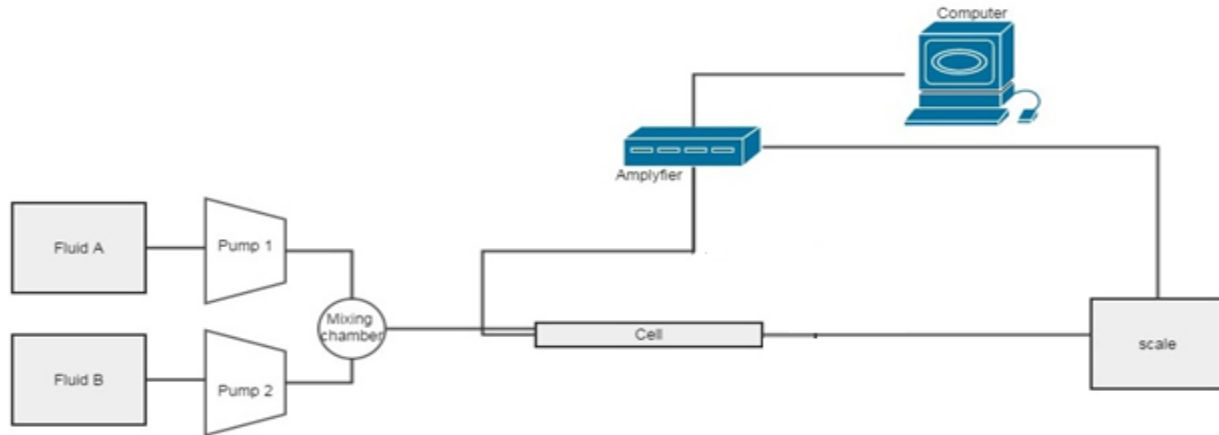


Figure 45 - The setup for precipitation test without heating

### Tools and equipment

Tools and equipment for the setup represented in Figure 45:

- Two container for both fluid A and fluid B.
- Two pumps with flow rate of 2 ml/min for each fluid (Figure 30).
- Mixing chamber
- Scale with ability of the connection to computer (Figure 35).
- VEE software to record pressure and flow rate.
- Pressure transducer for inlet with connection to computer.
- Amplifier for measurement of pressure and connecting to computer (Figure 34).
- A steel cell with 1.118cm diameter and 24 cm length (Figure 33).

### Process step by step:

1. Gravels were packed in the same procedure as explained in permeability test.
2. Mixture of 1.68 [g/lit] sodium bicarbonate in distilled water (fluid A). Mixture of 1.47 [g/lit] of calcium chloride in distilled water (fluid B).
3. Flow rate of two pumps are adjusted precisely on 2 [ml/min], to have a 50% mixture of each fluid in the mixing chamber.
4. Connect the cell to pressure transducer and pumps.
5. Place the cell in the vertical position and inject water to soak the grains.
6. Stop injecting water.
7. Set the pressure of the pressure transducer to zero.
8. Start injecting fluid A and B into the cell through mixing chamber.
9. Record the change in pressure and weight on the scale by VEE softer.
10. Calculate the flow rate by weight (on the scale), same as what have done in permeability test.

After several tests with long time injection of fluids, no change in the injection pressure was observed. It means, because of the high concentration, chemical reaction is fast in

homogeneous nucleation condition (without any need to preferential sites). Since nucleation is homogeneous and it does not adhere on the surface of grains, therefore all created crystals were produced.

#### 4.4.3.2 PRECIPITATION OF CALCIUM CARBONATE BY INCREASING THE TEMPERATURE-DYNAMIC SETUP

Since in the previous setup (Figure 45), precipitated calcium did not adhere on the surface of grains and it was concluded that nucleation was too quick so that all crystals were produced, the dynamic setup was modified to allow heating low concentration fluids.

Referring to the explanations in section 4.4.2, to make sodium bicarbonate and calcium chloride react and produce calcium carbonate in lower concentration of between 1 to 2 gr/lit, heating is necessary. Based on this evidence, to have a dynamic setup, two fluids with certain concentrations (1.68[gr/lit] for bicarbonate and 1.47[gr/lit] for calcium ion), mix and inject into the cell which is put in the heater (Figure 46).

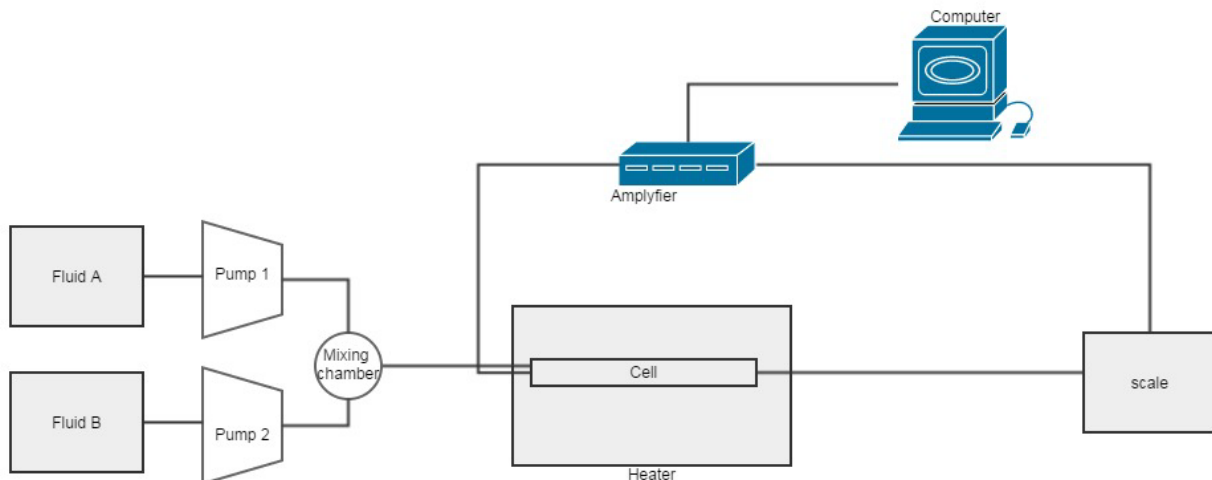


Figure 46 - Dynamic precipitation setup by heating.

Injection inlet pressure is measured to record increment of pressure because of precipitating and plugging the pore throat by  $\text{CaCO}_3$ .

Since the chemical reaction between sodium bicarbonate and calcium chloride start at temperature above  $40^\circ\text{C}$ , the test temperature was set to  $60^\circ\text{C}$ .

In addition a very slow flow rate for the precipitation blend was set to provide enough time for the chemical reaction inside the cell.

#### Tools and equipment

Tools and equipment for the setup represented in Figure 46:

- Two container for both fluid A and fluid B.
- Two pumps with flow rate of 2 ml/min for each fluid (Figure 30).
- Mixing chamber
- Heater with  $60^\circ\text{C}$  temperature (Figure 31)
- Scale with ability of the connection to computer (Figure 35).



- VEE software to record pressure and flow rate.
- Pressure transducer for inlet with connection to computer.
- Amplifier for measurement of pressure and connecting to computer (Figure 34).
- A steel cell with 1.118cm diameter and 24 cm length (Figure 33).

### Process step by step:

1. Gravels get packed in the same procedure as explained in permeability section.
2. Fluids get prepared. Mixture of 1.68 [g/lit] for sodium bicarbonate in distilled water (fluid A). mixture of 1.47 [g/lit] of calcium chloride in distilled water (fluid B).
3. Flow rate of two pumps are adjust precisely on 2 [ml/min] to have a 50% mixture of each fluid in the mixing chamber.
4. Connect the cell to pressure transducer and pumps.
5. First put the cell in the vertical condition and inject water to soak the grains.
6. Put the cell inside the hot heater and inject water until the outlet water get hot.
7. Stop injecting water.
8. Set the pressure of the pressure transducer into zero.
9. Start injecting fluid A and B into the cell through mixing chamber.
10. Record the change in pressure and weight on the scale by VEE softer.
11. Calculate the flow rate by weight (on the scale) same as what have done in permeability test.

### Results

The test results show, different time intervals and trends for scaling in various gravel packs.

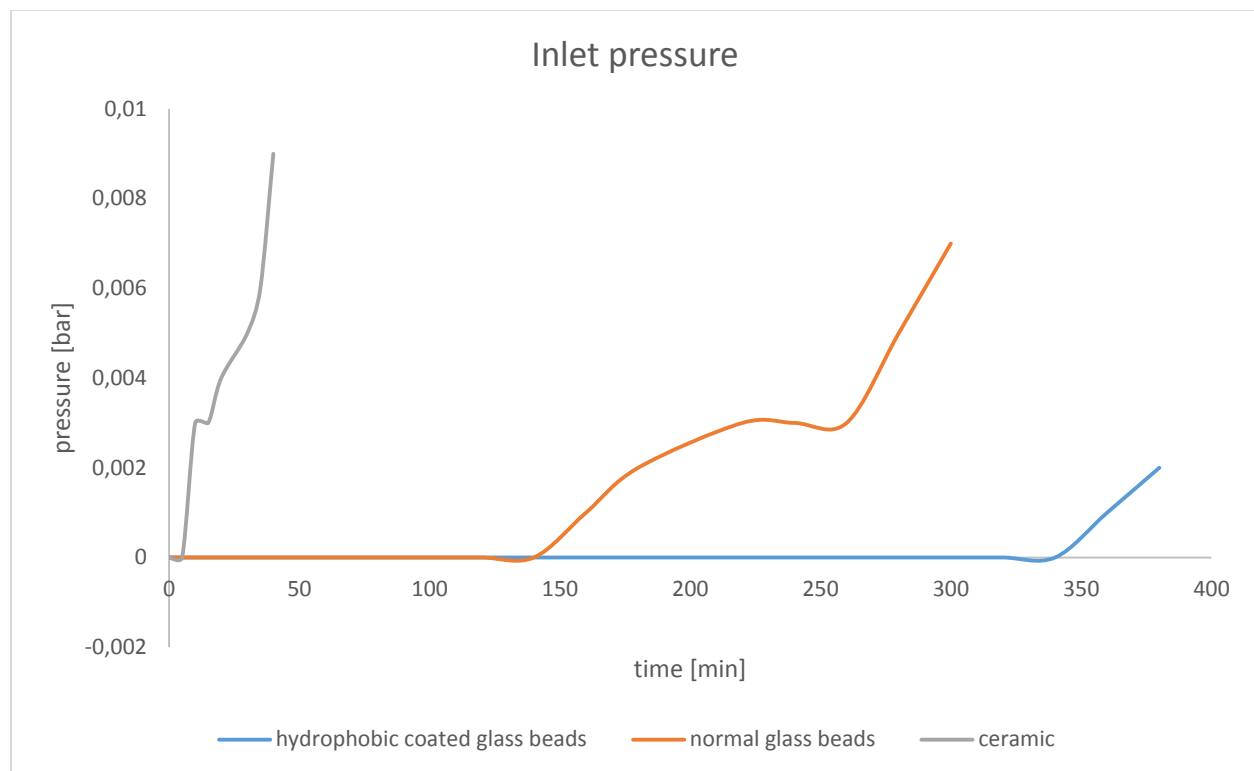


Figure 47 - The pressure increment because of calcium carbonate scaling.

As can be seen in Figure 47, in the first 30 minutes the scaling process was started on ceramic gravel packs. However it took 2 hours and 30 minutes to have calcium carbonate crystals on the surface of glass beads and this time even extended to 5 hours and 40 minutes in hydrophobic coated glass.

#### 4.4.4 MICROSCOPIC EVALUATIONS FOR DYNAMIC TEST

To confirm and investigate more thoroughly the results seen in the dynamic tests, the gravel pack material was looked at, under the microscope.

Figure 48 represents the microscopic picture of one ceramic grain after the dynamic precipitation test. As can be seen the scale crystals are distributed all over the ceramic grain. The picture perfectly shows the adherence of scale on the grain's surface. The photo proves the results deduced from dynamic test.

Because of the roughness of ceramic grain's surface, in some parts it was difficult to distinguish between original surface of grain and scale. Therefore Figure 49 magnified the surface and perfectly shows the crystals of calcium carbonate on the surface of ceramic grain.

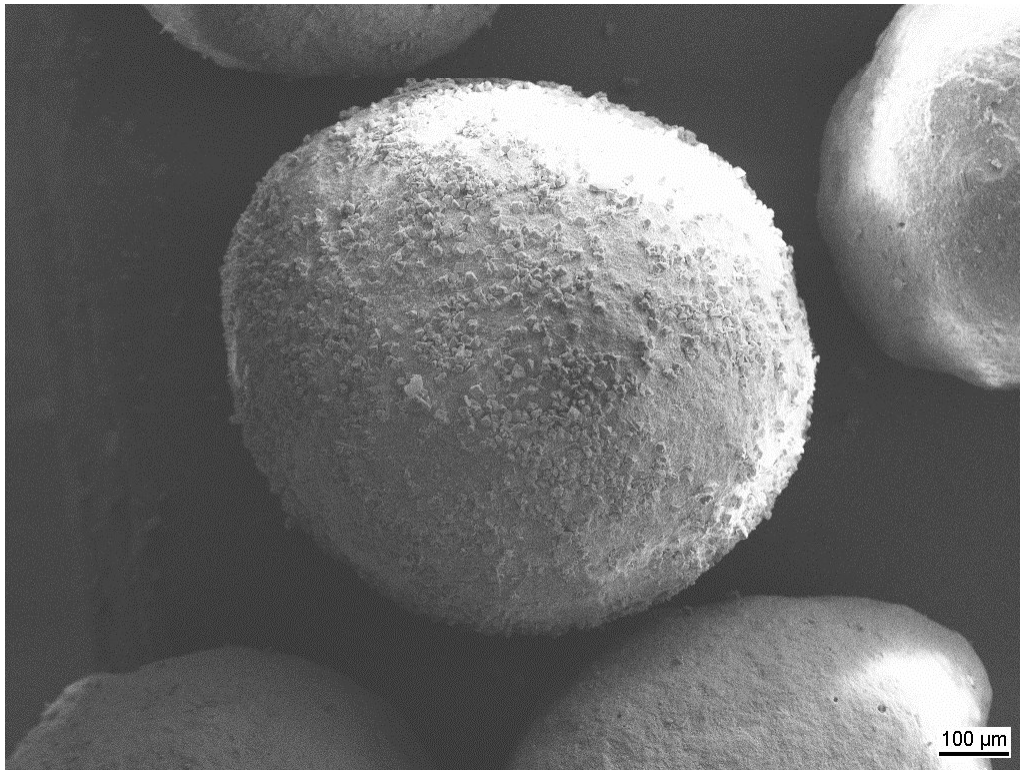


Figure 48 - Ceramic grain after dynamic precipitation test in 60° centigrade.

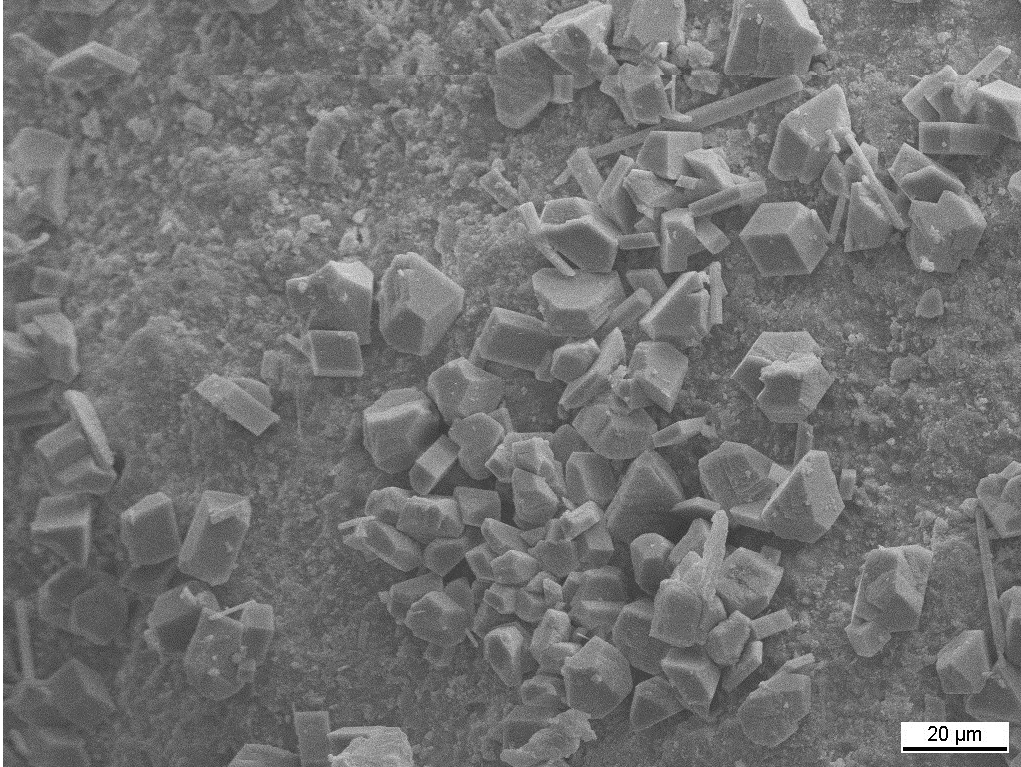


Figure 49 - Calcium carbonate crystal on the surface of ceramic after dynamic precipitation test at 60° centigrade.

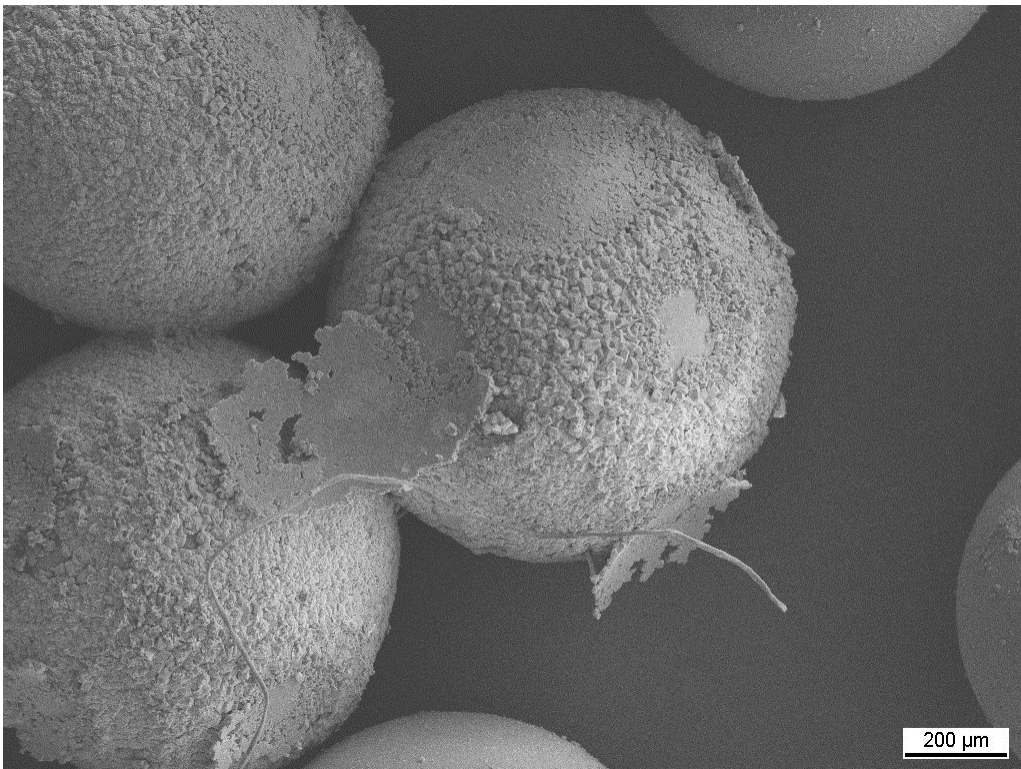


Figure 50 - Precipitation and adherence of calcium carbonate on the surface of glass grain in dynamic test at 60° centigrade.

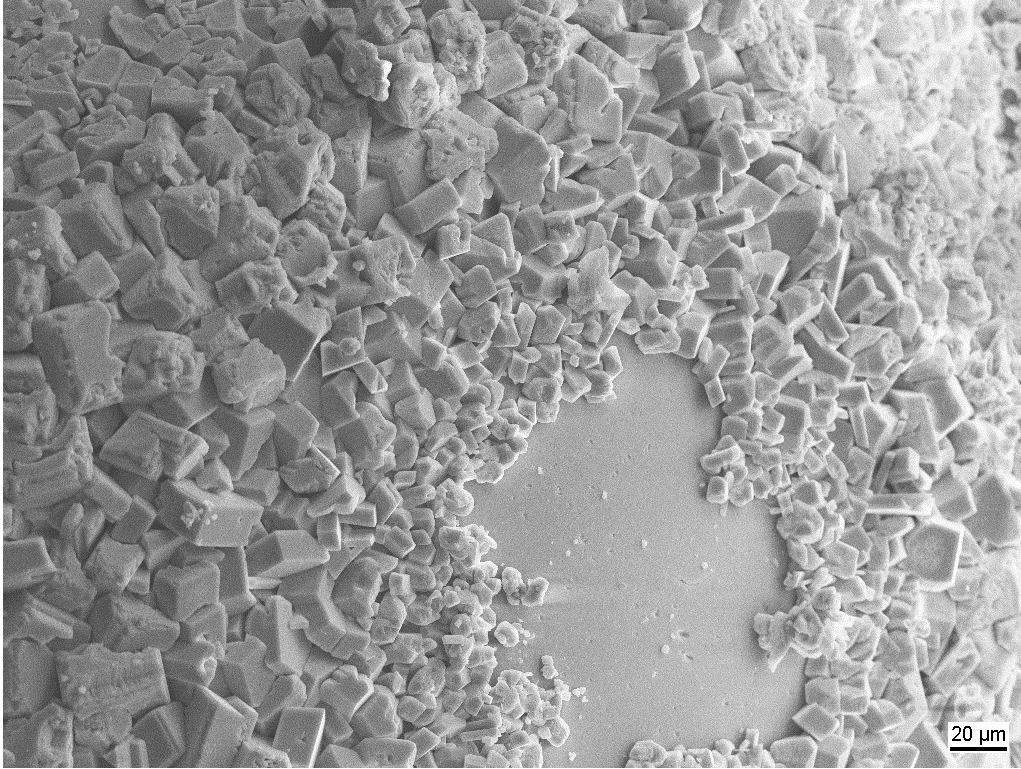


Figure 51 - Precipitation of calcium carbonate on the surface of glass in dynamic test at 60° centigrade.

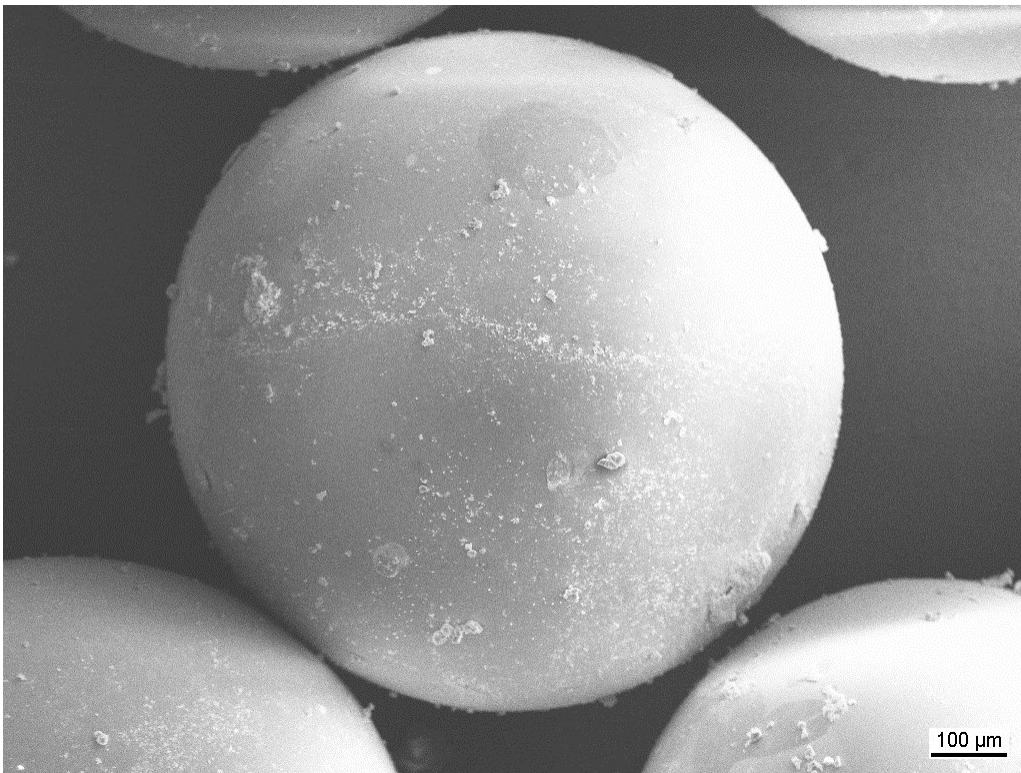


Figure 52 - Hydrophobic glass picture after dynamic precipitation test in 60° centigrade.

Figure 50 and Figure 51, clearly show the adherence of calcium carbonate on the surface of glass beads. However Figure 52 demonstrates that much less calcium carbonate adhered to the surface of hydrophobic coated glass beads compared to the non-coated glass beads.

#### 4.4.5 MICROSCOPIC EVALUATION OF STATIC TEST

Although dynamic testing is the best way to simulate the downhole condition in the laboratory, static test has been done in this research as supplementary experimental information.

The procedure of static test is as follow:

- 5 gr of each grain samples (ceramic, glass, hydrophobic coated glass) provided.
- Mixture of 1.68 [gr/lit] of sodium bicarbonate in distilled water prepared.
- Mixture of 1.47 [gr/lit] of calcium chloride in distilled water prepared.
- Both fluids were mixed in a 50% mixture (volumetric 50% mixture of two fluids).
- 200 cc of 50% mixture was added to the samples.
- Samples were heated up in the oven for 7 days at 80 °C.
- After a week, samples were dried and prepared to be evaluated under microscope.

The Figure 53, Figure 55 and Figure 56 respectively represent the crystallization of calcium carbonate in the static condition on the surface of ceramic, glass and hydrophobic coated glass beads.



Figure 53 - Crystallization of calcium carbonate on the surface of ceramic grain after static test.

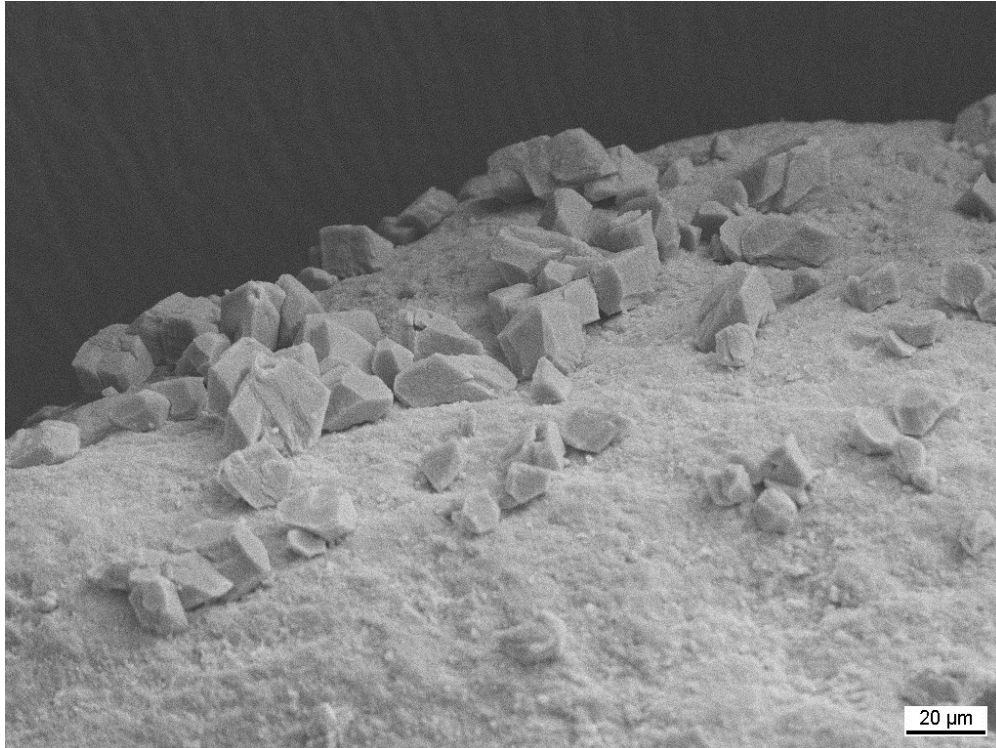


Figure 54 - Microscopic picture of surface of ceramic grain after static precipitation test.

Large crystals can be seen on the surface of ceramic but also as it represents in Figure 54 there are small crystals on the smooth surfaces either.

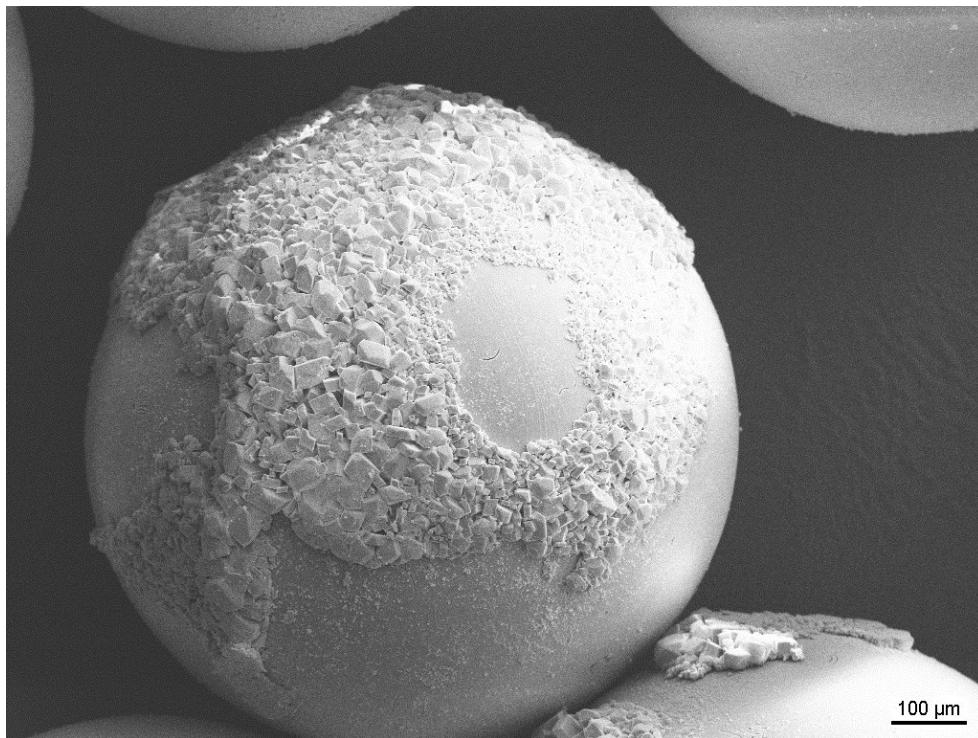


Figure 55 - Non-coated glass bead after static test.

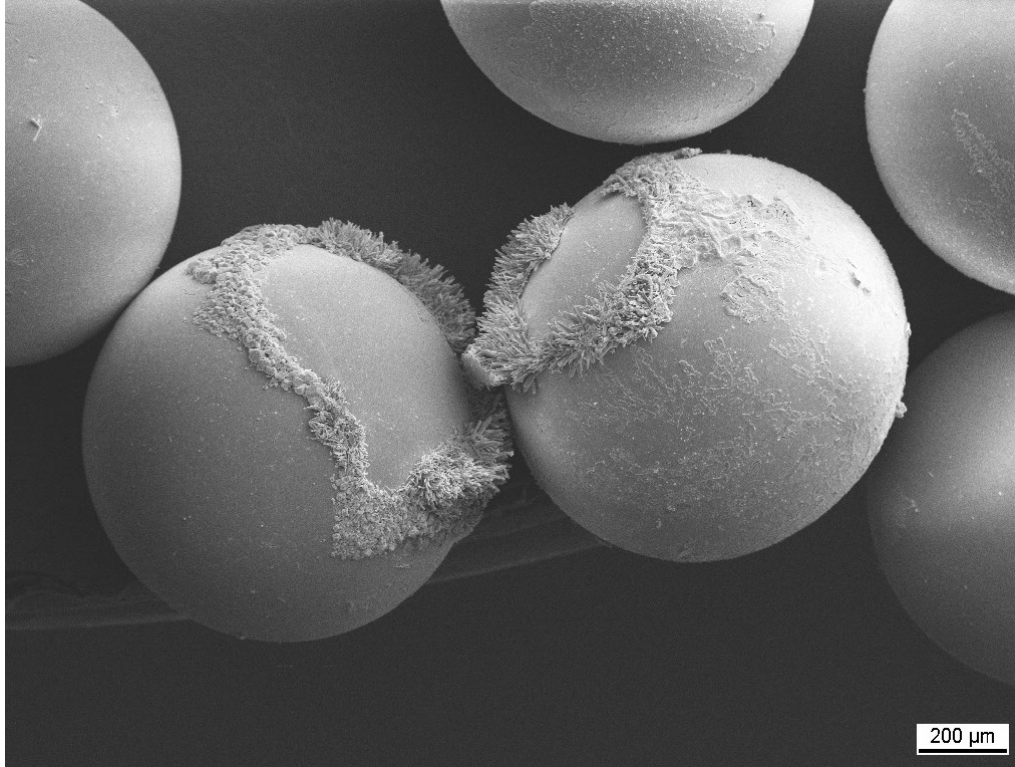


Figure 56 - Microscopic photo of hydrophobic coated glass bead after static precipitation test.

As can be seen in the photos, ceramic has the highest amount of scale between samples and hydrophobic coated glass beads shows the lowest adherence on its surface.

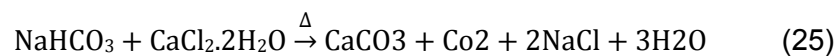
#### 4.4.6 DISCUSSION

Although all of the different filter mediums tested in the dynamic and static scaling test, showed adherence of carbonate scale on their surfaces, it was experienced that the time in which the scaling occurred was very different. Because of the smoothness and hydrophobicity of the tested glass beads the scale adherence to the grains was effectively deferred.

During the testing, three parameters were significantly influenced the scaling rate: 1.) length of the cell, 2.) Temperature and 3.) Concentration of solutions

The importance of concentration which is described in detail in section 4.4.2, is given by the fact that too high concentrations do not provide realistic results since the crystallisation is too rapid and therefore scale does not have time to adhere on the surfaces. In the contrary, too low concentrations might require too much time before scaling starts and therefore time is not practical. Solution concentrations of 1 [gr/ltr] to [2 gr/ltr] of each salt provided acceptable times of scaling initiation in this laboratory setup.

Temperature is also important because the formation of carbonate scale as described in the reaction equation (equation 25) need thermal energy.



In regards to the temperature it was seen that the length of the flow cell was important because the solutions need to remain long enough inside the filter medium pack to absorb enough energy for scale formation. This phenomena was experienced when ceramic gravel was tested in a temperature of 60°C in two different cells. One was 24 cm long while the other cell only 4 cm. Figure 57 shows the results and it can be seen that in the shorter cell scale did not precipitate.

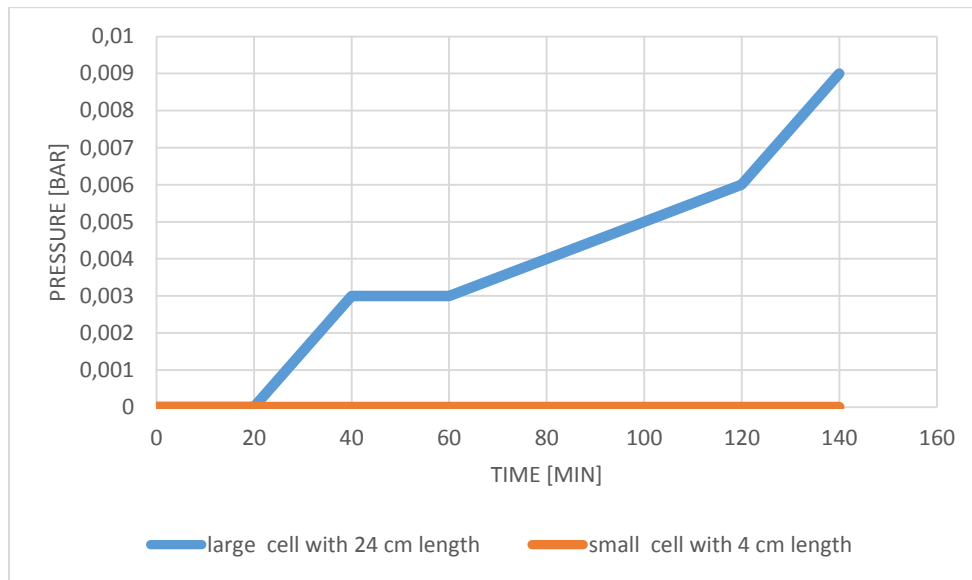


Figure 57 - Effect of length on nucleation along the cell.



## 5 CONCLUSION AND FUTURE DIRECTIONS

The study was set out to explore the concept of scaling phenomena in gravel packing system. In this regard hydrophobic coated and non-coated glass and ceramic gravels were compared to each other. Main conclusions are presented in the following:

### 5.1 CONCLUSION

First step of this research is evaluation of the gravel's physical properties. In comparison with other materials like natural quartz sand and ceramic proppants, glass beads are very well sorted and, because of narrow size distribution and roundness. A glass beads pack demonstrated a significantly higher permeability than commercialized ceramic proppant or quartz sand. The permeability of the glass beads pack was almost two times higher than the manmade ceramic proppants.

To evaluate scaling trends on glass beads, the study sought to explain the theory behind the scaling in the experiments and effective factors in this phenomena.

Scaling theoretically explained by Gibbs free energy. Based on this theory to create the initial crystals, since the differentiation of Gibbs energy is positive, chemical reaction need thermal energy. Therefore the chemical reaction, which triggers the formation of crystals needs thermal energy, because the difference of Gibbs energy is positive. But when the crystals grow to a certain volume, they exceed a critical radius, the Gibbs energy gets negative, which means, that the growth of crystal is not anymore depended on thermal energy, but the soluble material in the water. This phenomena is described in more detail in Appendix A. The tests demonstrated that scaling happens in all examined gravel pack materials despite of their form and surface (Figure 47). Nevertheless the tests clearly showed that the time interval in which nucleation on smooth and treated surfaces occur and crystals start growing fast is longer.

Those scales that adhered and growth on the surface of gravels (heterogeneous nucleation), impact on the permeability reduction of gravel pack. In this regards, the more rough and imperfect sites on the surface of gravels, the less Gibbs free energy is needed to create calcium carbonate crystals( for more information see Appendix A ). Rough surface and imperfect sites on the ceramic gravels in comparison to glass, makes the scaling easier and faster on the surface of ceramic gravels.

In addition hydrophobic coating material on the surface of glass, avoid the contact between glass surface and water phase which reduce the possibility of scaling.

Although scale was formed on all types of gravel packs, the tendency of scale adhering on smooth surfaces such as glass beads and especially hydrophobic coated glass is significantly reduced.

### 5.2 FUTURE DIRECTIONS

The most interesting topic to extend the scope of this study is to experiment sand invasion phenomena with glass beads. This interest aroused by the phenomena described in section 3.1, preferred range for gravel sizing is to use gravels with 5 to 6 times larger than formation sands. But even in this range there is a shallow sand invasion. Based on mathematical calculations to avoid formation sands from invading the gravel pack pore throats, the ratio of gravel to sand should be around 3.5. This ratio is calculated based on considering uniform gravel sizes while

variable size distribution in normal gravels increase this ratio. As a result, utilization of glass beads with a very narrow size distribution could probably reduce the sand invasion.

Another dimension that was not examined in this study is the effect of two phase flowing condition throughout hydrophobic coated gravel pack. During two phase production, generally in hydrophilic or water wet gravel packing, the water saturation at bottom hole increase because of water absorbing on the surface of gravels. This increment in water saturation can decrease oil production or water blocking. Probably hydrophobic layer on the surface of gravels, let higher amount of water to produce and possibility of water blockage at the bottom hole could be reduced.

## 6 REFERENCES

- [1] A. M. et.al, "Comparative Study of Sand Control Methods," October 2012.
- [2] C.H.Rawlins, "A Comparison of Methodologies for Handling Produced Sand and Solids to Achieve Sustainable Hydrocarbn Production," *SPE 107690*, 2007.
- [3] M. B. a. al, "Improved Selection Criteria for Sand Control - When Are "Fines"Fines?," *SPE 128038*, 2010.
- [4] j. c. et.al, "Sand Control:Why and How?," p. 2, October 1992.
- [5] T. O. a. AlanP.Robert, "Sand control," in *Production Operation*, 1982, p. 36.
- [6] A. Acock, "practical approach to sand management-Oil field review," 2004.
- [7] A. e. al, "Sand Control: Sand characterization, Failur mechanisms and completion methods," *SPE 77686*, 2002.
- [8] M.B.Geilikman, "Bean-Up Guildlines for Sand control Completions," *SPE 95870*, 2005.
- [9] M. O. a. J. H.-W. U. Yann Bigno, "Investigation of Pore Blocking Mechanism in gravel packs in the Management and Control of Fines Migiration," *SPE 27342*, 1994.
- [10] D. E. P. M.Crbtree, "Fighting Scale-removal and prevention," 1999.
- [11] K.D.Carrell, "The Occurence , Prevention and Treatment of Sulphate," *SPE 16538/1*, 1987.
- [12] R. Jasinski, "Calcite Scaling Tendencies for North Sea HTHP Wells: Prediction, Authentication and Application," *SPE 49198*, vol. 2, 1998.
- [13] G. Loewrnthal. R.E and Marias, *Carbonate Chemistry of Aquatic Systems: Theory and Applications*, vol. 1, 1978.
- [14] P. Y. Duggirala, "Formation of Calcium Carbonate Scale and Control Strategies in Continuous Digesters".
- [15] M. Kapelke, "Prevention of Calcium Carbonate Precipitation From Calcium Chloride Kill Fluid in CO2-Laden Formations," *SPE 12752*, 1982.
- [16] O. V. & W.A.Farone, "Calcium Carbonate Scale Considerations: A Practical Approach," *SPE 17009*, 1987.
- [17] J. & P. Nguyen, "Hydrophobic Filming Reduces Frac Gel and Mineral Scale Damage," *SPE 138314*, 2010.
- [18] H. e. al, "Surfactants and Polymers in Aqueous Solutio," 2002.
- [19] M.Ukrainczyk, "Precipitated Calcium Carbonate Prepared by Batch and Semicontinuous Processes," 2007.
- [20] D. A. C. Zidovec, "Dynamic Method to Measure Calcium Carbonate Scaling," *99111 NACE Conference Paper*, 1999.
- [21] N. e. a. Fleming, "Controlled Use of Downhole Calcium Carbonate Scaling for Sand Control: Laboratory & Field Results, Gullfaks," *SPE 144047*, 2011.
- [22] A. e. al, "Production Enhancement From Sand Management Philosophy:A case study from statfjord and gullfaks," *SPE 94511*, 2005.
- [23] H. e. al, "Sand Production Prediction and the selection of completion methods for horizontal wells in Intercompo oilfield, Venezuela," *SPE 93821*, 2005.

- [24] R. e. al, "Successful applications of expandable sand screen in persian oil field," *SPE* 133364, 2010.
- [25] C.R.Marek, *Importance of Fine Aggregate Shape and Grading on Properties of Concrete*.
- [26] F.F.Abraham, "Academic Press, NY," *Homogeneous nucleation theory*, 1974.
- [27] R. P.Sear, *Nucleation: Theory and Applications to Protein Solutions and Colloidal Suspension*, 2006.



## 7 APPENDICES

### 7.1 APPENDIX A

**Nucleation:** is a localized formation of a distinct thermodynamic phase that result forming nucleus or clusters. In this process ions, atoms or molecules forming a crystalline solids. Formation of gaseous bubbles or crystals in liquid or creation of liquid droplet in saturated vapour are some examples that occur in nature.

**Homogeneous nucleation:** occur spontaneously and randomly without preferential nucleation sites but need superheating or supercooling of medium.

Super cooling or superheating causes super saturation or in the other word by changing the thermodynamic condition change the saturation limit and as a result nucleation occur. Super saturation occur when the pressure in a newly formed solid is less than liquid pressure and result changing in free energy per unit volume between liquid and newly created solid phase.

The free energy has two part, one is the energy released by creation of cluster and the other is energy needed for surface interfacing that is related to radius of cluster. Then for a spherical cluster we have:

$$\Delta G = \frac{4}{3}\pi r^3 \Delta G_v + 4\pi r^2 \sigma$$

Where first term is the energy gained or released by creation of cluster and the second term is the energy need or energy loss because of surface tension ( $\sigma$ ) of new cluster. Until  $\Delta G$  is positive, it cost free energy to add molecules to this cluster but as can be seen at Figure 58 when the cluster's radius reach to critical radius the difference of free energy start to decrease and getting negative so increment or growth of the cluster's radius is no longer limited by nucleation and occurring automatically and the only thing that can stop it is the supply of

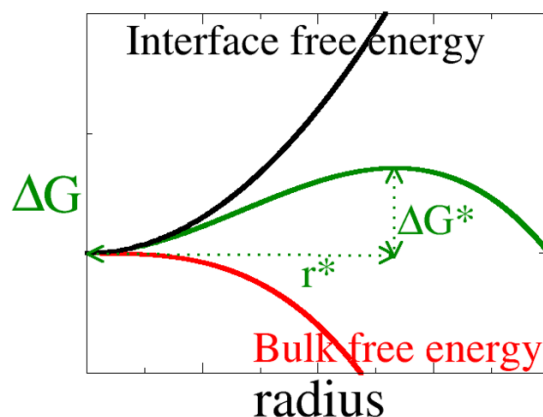


Figure 58 - The green curve is the total (Gibbs if this is at constant pressure) free energy as a function of radius. Shown is the free energy barrier,  $\Delta G^*$ , and radius at the top of the barrier,  $r^*$ . The bulk free energy is the one that release because of creation of new volume and plotted in red. The interface free energy is always positive and represent the energy is needed to change the interfacial energy and plotted in black [26]

molecules.

The critical radius is calculated when  $\frac{dG}{dr} = 0$ :

$$r^* = -\frac{2\sigma}{\Delta G_v}$$

**Heterogeneous nucleation:** This process applies to the phase transformation between any two phases of gas, liquid or solid and clusters forms at preferential sites like phase boundaries, surfaces or impurities such as dust, because at such a preferential sites the effective surface energy is lower and less energy barrier ( $\Delta G^*$ ) causes the process be done faster. In homogenous nucleation the clusters are spherical and has a surface energy equal to sphere area which is  $4\pi r^2$  times surface tension however for heterogeneous nucleation droplets on the surfaces are not in complete spherical shape so the interfacial area and therefore interfacial free

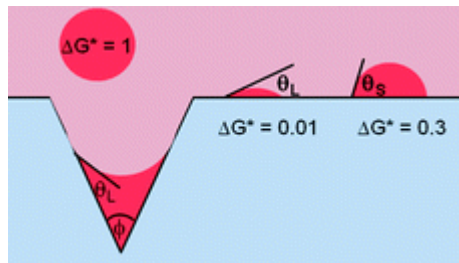


Figure 59- Schematic of heterogeneous nucleation according to classical nucleation theory with the relative magnitudes of the energy barrier compared to homogeneous nucleation and capillary condensation in a wedge.  $\Delta G^* = 0.3$  corresponds to a contact angle of about  $75^\circ$  and  $\Delta G^* = 0.01$  to a contact angle of about  $30^\circ$  [27]

energy reduces (Figure 59). So heterogeneous nucleation is a function of contact angle.

$$\Delta G_{heterogeneous} = \Delta G_{homogeneous} \times f(\theta)$$

## 7.2 APPENDIX B

Shape classification:

The concept of particle's shape is based on three geometrical idea: sphericity, roundness and form. Sphericity is a measure of how nearly equal are the three axes or dimensions of a particle. Roundness represent the sharpness of the edges and corners of a particle. Form is a measure of the relation between the three dimensions of a particle based on ratios between the proportions of the long (a), medium (b) and the short (c) axes of the particle. Form also referred as shape factor.

Shape factor is describe in terms of ratios as follows:

$$\begin{aligned} \text{Elongation ratio} &= q = b/a \\ \text{Flatness ratio} &= p = \frac{c}{b} \\ \text{Shape factor} &= F = \frac{p}{q} = ac/b^2 \end{aligned}$$

A graphical representation of various shape categories is given in Figure 60. Sphericity and roundness evaluation is obtain by numerical values by visual approximation comes from Figure 61 .

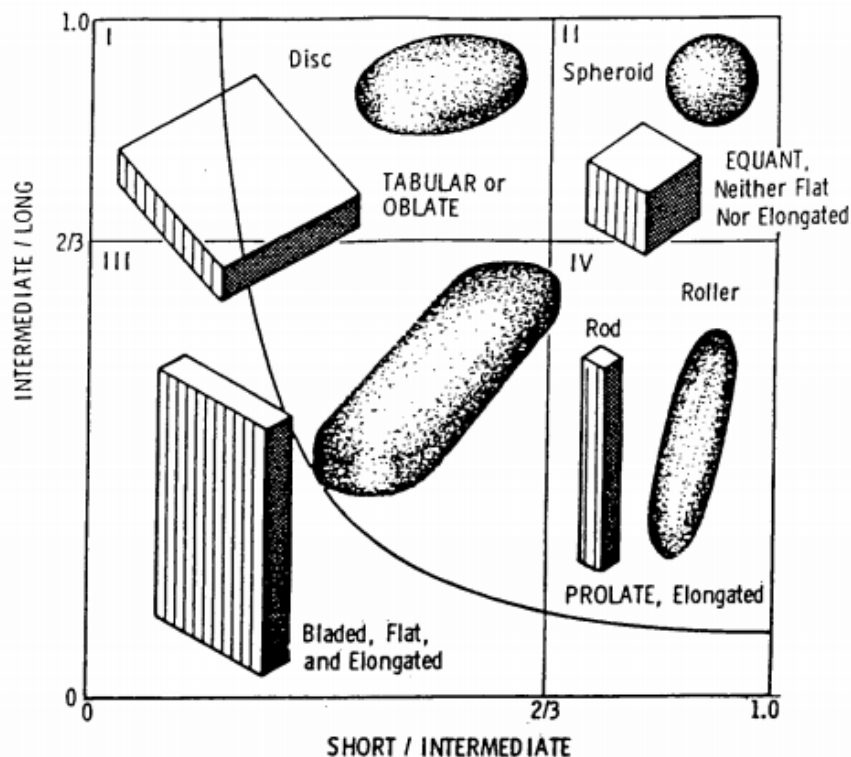


Figure 60 - Shape categories defined by ratio of two thirds for  $b/a$  and  $c/b$  [25].



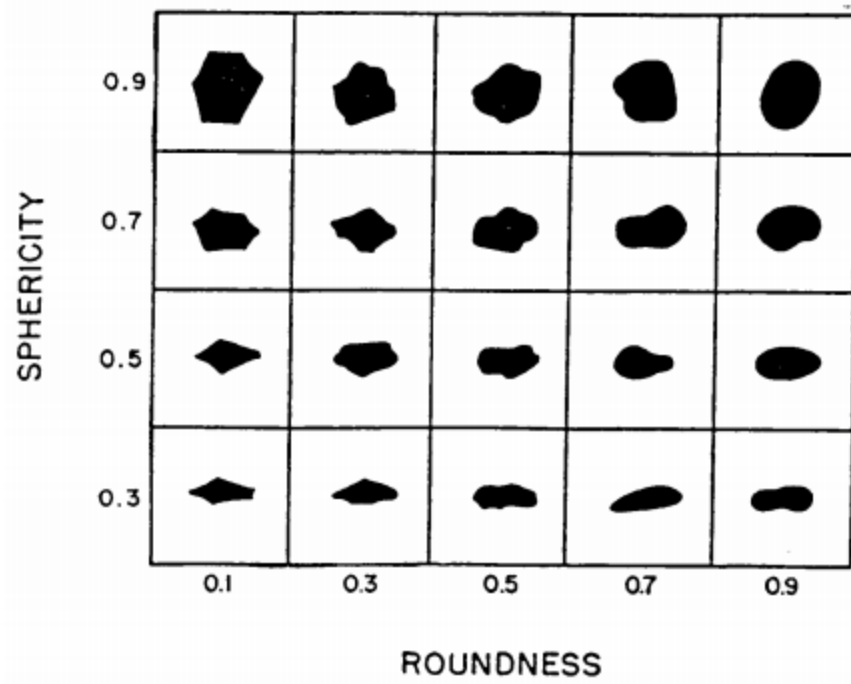


Figure 61 - Visual chart for estimation of roundness and sphericity of particles [25]

